

# Strong decay properties of single heavy baryons $\Lambda_Q$ , $\Sigma_Q$ and $\Omega_Q$

Guo-Liang Yu<sup>1,\*</sup>, Yan Meng<sup>1</sup>, Zhen-Yu Li<sup>2</sup>, Zhi-Gang Wang<sup>1,†</sup> and Lu Jie<sup>1</sup>

<sup>1</sup> *Department of Mathematics and Physics, North China Electric Power University,  
Baoding 071003, People's Republic of China*

<sup>2</sup> *School of Physics and Electronic Science, Guizhou Education University,  
Guiyang 550018, People's Republic of China*

(Dated: May 9, 2023)

Motivated by recent progresses in experiments in searching for the  $\Omega_c$  baryons, we systematically analyze the strong decay behaviors of single heavy baryons  $\Lambda_Q$ ,  $\Sigma_Q$  and  $\Omega_Q$ . The two-body strong decay properties of  $S$ -wave,  $P$ -wave and some  $D$ -wave states are studied with the  ${}^3P_0$  model. The results support assigning the recently observed  $\Omega_c(3185)$  and  $\Omega_c(3327)$  as the  $2S(\frac{3}{2}^+)$  and  $1D(\frac{3}{2}^+)$  states, respectively. In addition, the quantum numbers of many other experimentally observed baryons are also suggested according to their strong decays. Finally, some baryons which have good potentials to be observed in experiments are predicted and the possible decay channels for searching for these predicted states are also suggested.

PACS numbers: 13.25.Ft; 14.40.Lb

## 1 Introduction

Very recently, two new excited states,  $\Omega_c(3185)$  and  $\Omega_c(3327)$ , were observed in the  $\Xi_c^+ K^-$  invariant-mass spectrum using proton-proton collision data collected by the LHCb experiment, corresponding to an integrated luminosity of  $9\text{fb}^{-1}$ [1]. At the same time, another five previously observed  $\Omega_c$  states,  $\Omega_c(3000)$ ,  $\Omega_c(3050)$ ,  $\Omega_c(3065)$ ,  $\Omega_c(3090)$ ,  $\Omega_c(3119)$ [2] were also confirmed. Actually, scientists have made great progresses in searching for the single heavy baryons such as  $\Lambda_c(2595)$ [3],  $\Lambda_c(2625)$ [4, 5],  $\Lambda_c(2765)$ [6],  $\Lambda_c(2940)$ [7–9],  $\Lambda_b(5912)$  and  $\Lambda_b(5920)$ [10, 11],  $\Lambda_b(6072)$ [12],  $\Lambda_b(6146)$  and  $\Lambda_b(6152)$ [13],  $\Sigma_c(2800)$ [14],  $\Sigma_b(6097)$ [15],  $\Omega_b(6330)$ ,  $\Omega_b(6316)$ ,  $\Omega_b(6350)$  and  $\Omega_b(6340)$ [16]. All of the experimentally discovered  $\Lambda_Q$ ,  $\Sigma_Q$  and  $\Omega_Q$  baryons are collected in Tables I-III. The quantum numbers of some baryons have been suggested or confirmed, however the others are still unidentified.

In our previous work, we have systematically studied the mass spectra of the  $\Lambda_Q$ ,  $\Sigma_Q$  and  $\Omega_Q$  systems with the constituent quark model[17]. The quantum numbers of the experimentally observed baryons were suggested and are also shown in Tables I-III. At the same time, some excited baryon states were also predicted in Ref.[17]. For example, the predicted masses are 3197 MeV for the  $2S(\frac{3}{2}^+)$   $\Omega_c$  baryon and 3304–3315 MeV for the  $1D$  ones. These results are consistent well with the

---

\*Electronic address: [yuguoliang2011@163.com](mailto:yuguoliang2011@163.com)

†Electronic address: [zgwang@aliyun.com](mailto:zgwang@aliyun.com)

experimental data of the newly observed  $\Omega_c(3185)$  and  $\Omega_c(3327)$  baryons. This implies that these two baryons can be assigned as the  $2S(\frac{3}{2}^+)$  and  $1D$  states, respectively. In addition, many other states which have good potentials to be found in experiments were predicted, such as the  $2P \Lambda_c(\frac{3}{2}^-)$ ,  $2P \Lambda_b$  doublet  $(\frac{1}{2}^-, \frac{3}{2}^-)$ ,  $1P \Sigma_c/\Sigma_b$ , and  $1D \Omega_b$  states[17]. To make a further confirmation about the assignments of the experimental states and provide more valuable information for searching for these predicted baryons, it is necessary to systematically investigate the strong decay behaviors of the single heavy baryons. Fortunately, we can continue this research now with the results obtained from the quark model[17].

As a phenomenological method, the  $^3P_0$  quark model was developed to study the OZI-allowed hadronic decay widths[18–26]. Now, this model has been extensively used to describe the two-body strong decays of the heavy mesons in the charmonium and bottomonium systems[27–40], the baryons[41–57] and even the tetraquark states[58]. In this work,  $^3P_0$  model will be employed to study the two-body strong decay properties of the  $S$ -wave,  $P$ -wave and some  $D$ -wave single heavy baryons. The calculated strong decay widths in this work will be confronted with the experimental data in the future and will be helpful in searching for new states of single heavy baryons from the Belle, BABAR, CLEO and LHCb collaborations.

The paper is organized as follows. In Section II, we give a brief review of the  $^3P_0$  decay model; In Sec III, using the predicted mass spectra by quark model[17], we study the two-body strong decay behaviors of the  $S$ -wave,  $P$ -wave and some  $D$ -wave heavy baryon states. And Sec IV is reserved for our conclusions.

## 2 $^3P_0$ strong decay model

The main idea of  $^3P_0$  model is that the strong decay takes place via the creation of a  $^3P_0$  quark-antiquark pair from the vacuum. Then, this quark-antiquark pair regroups with the initial hadron A into two daughter hadrons B and C. This process is illustrated in Fig. 1.

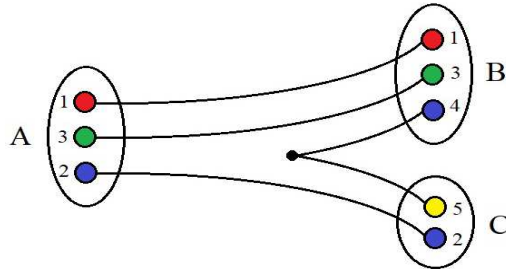


FIG. 1: The decay process of  $A \rightarrow B + C$  in the  $^3P_0$  model.

In the  ${}^3P_0$  model, the strong decay width for the process  $A \rightarrow B + C$  can be written as[41, 45–47],

$$\Gamma = \pi^2 \frac{|\mathbf{p}|}{m_A^2} \frac{1}{2J_A + 1} \sum_{M_{J_A} M_{J_B} M_{J_C}} |M^{M_{J_A} M_{J_B} M_{J_C}}|^2, \quad (1)$$

where  $m_A$  and  $J_A$  are the mass and total angular momentum of the initial baryon A,  $m_{B(C)}$  and  $J_{B(C)}$  are the ones for the daughter hadrons.  $|\mathbf{p}| = \frac{\sqrt{[m_A^2 - (m_B - m_C)^2][m_A^2 - (m_B + m_C)^2]}}{2m_A}$  is the momentum of the daughter hadrons in the centre-of-mass frame.  $M^{M_{J_A} M_{J_B} M_{J_C}}$  in Eq.(1) is the helicity amplitude, which reads[41, 45–47]

$$\begin{aligned} & M^{M_{J_A} M_{J_B} M_{J_C}} \\ &= -F\gamma\sqrt{8E_A E_B E_C} \sum_{m_{l_{\rho A}} M_{L_A}} \sum_{m_{l_{\rho B}} M_{L_B}} \sum_{m_{s_1}, m_{s_3}, m_{s_4}, m} \sum_{\langle j_A m_{j_A} s_3 m_{s_3} | J_A M_{J_A} \rangle} \\ & \quad \times \langle l_{\rho A} m_{l_{\rho A}} l_{\lambda A} m_{l_{\lambda A}} | L_A M_{L_A} \rangle \langle L_A M_{L_A} S_{12} M_{S_{12}} | j_A m_{j_A} \rangle \langle s_1 m_{s_1} s_2 m_{s_2} | S_{12} M_{S_{12}} \rangle \\ & \quad \times \langle j_B m_{j_B} m_3 m_{m_3} | J_B M_{J_B} \rangle \langle l_{\rho B} m_{l_{\rho B}} l_{\lambda B} m_{l_{\lambda B}} | L_B M_{L_B} \rangle \langle L_B M_{L_B} S_{14} M_{S_{14}} | j_B m_{j_B} \rangle \\ & \quad \times \langle s_1 m_{s_1} s_4 m_{s_4} | S_{14} M_{S_{14}} \rangle \langle 1m; 1-m | 00 \rangle \langle s_4 m_{s_4} s_5 m_{s_5} | 1-m \rangle \\ & \quad \times \langle L_C M_{L_C} S_C M_{S_C} | J_C M_{J_C} \rangle \langle s_2 m_{s_2} s_5 m_{s_5} | S_C M_{S_C} \rangle \times \\ & \quad \times \langle \varphi_B^{1,4,3} \varphi_C^{2,5} | \varphi_A^{1,2,3} \varphi_0^{4,5} \rangle \times I_{M_{L_B}, M_{L_C}}^{M_{L_A}, m}(\mathbf{p}). \end{aligned} \quad (2)$$

In the above equation,  $\mathbf{s}_i$  is the spin of the  $i$ th quark,  $\mathbf{l}_\rho$  and  $\mathbf{l}_\lambda$  denote the orbital angular momentum between two light quarks, and between the heavy quark and light quark subsystem(Fig. 2), respectively.  $\mathbf{L}$  is the total orbital angular momentum,  $\mathbf{j}$  represents total angular momentum of  $\mathbf{L}$  and the total spin  $\mathbf{S}_{ij}$  of the light quark subsystem,  $\mathbf{J}$  is the total angular momentum of a baryon. The Clebsch-Gordan coefficients in Eq.(2) indicate the conservation of the angular momentum, *e.g.*,  $\mathbf{s}_1 + \mathbf{s}_2 = \mathbf{S}_{12}$ ,  $\mathbf{l}_{\rho A} + \mathbf{l}_{\lambda A} = \mathbf{L}_A$ ,  $\mathbf{S}_{12} + \mathbf{L}_A = \mathbf{j}_A$  and  $\mathbf{s}_3 + \mathbf{j}_A = \mathbf{J}_A$ .  $F$  is a factor equal to 2 when each one of the two quarks in C has isospin  $\frac{1}{2}$ , and  $F = 1$  when one of the two quarks in C has isospin 0[21, 46].  $\langle \varphi_B^{1,4,3} \varphi_C^{2,5} | \varphi_A^{1,2,3} \varphi_0^{4,5} \rangle$  is the flavor matrix element of the flavor wave functions  $\varphi_i$  ( $i=A, B, C, 0$ ), which has the following relation with the isospin matrix element  $\langle I_B I_B^3 I_C I_C^3 | I_A I_A^3 \rangle$ [21, 45],

$$\langle \varphi_B^{1,4,3} \varphi_C^{2,5} | \varphi_A^{1,2,3} \varphi_0^{4,5} \rangle = \mathcal{F}^{(I^A, I^B, I^C)} \langle I_B I_B^3 I_C I_C^3 | I_A I_A^3 \rangle, \quad (3)$$

where

$$\mathcal{F}^{(I^A, I^B, I^C)} = f \times (-1)^{I_{13} + I_C + I_A + I_2} \times \left[ \frac{1}{2} (2I_C + 1)(2I_B + 1) \right]^{1/2} \times \begin{Bmatrix} I_{13} & I_B & I_4 \\ I_C & I_2 & I_A \end{Bmatrix}. \quad (4)$$

Here,  $I_A$ ,  $I_B$  and  $I_C$  represent the isospins of the initial baryon, the final baryon and the final meson.  $I_{13}$ ,  $I_2$  and  $I_4$  denote the isospins of relevant quarks, respectively.  $f$  takes the value  $f = (\frac{2}{3})^{1/2}$  if the isospin of the created quark is  $\frac{1}{2}$ , and  $f = -(\frac{1}{3})^{1/2}$  for the isospin of 0[21, 46]. In Eq.(2), the space

integral is written as[41, 45–47],

$$\begin{aligned}
I_{M_{L_B}, M_{L_C}}^{M_{L_A}, m}(\mathbf{p}) &= \int d\mathbf{p}_1 d\mathbf{p}_2 d\mathbf{p}_3 d\mathbf{p}_4 d\mathbf{p}_5 \delta^3(\mathbf{p}_1 + \mathbf{p}_2 + \mathbf{p}_3 - \mathbf{p}_A) \delta^3(\mathbf{p}_4 + \mathbf{p}_5) \\
&\times \delta^3(\mathbf{p}_1 + \mathbf{p}_4 + \mathbf{p}_3 - \mathbf{p}_B) \delta^3(\mathbf{p}_2 + \mathbf{p}_5 - \mathbf{p}_C) \Psi_B^*(\mathbf{p}_1, \mathbf{p}_4, \mathbf{p}_3) \Psi_C^*(\mathbf{p}_2, \mathbf{p}_5) \\
&\times \Psi_A(\mathbf{p}_1, \mathbf{p}_2, \mathbf{p}_3) y_{lm}\left(\frac{\mathbf{p}_4 - \mathbf{p}_5}{2}\right). \tag{5}
\end{aligned}$$

where  $\mathbf{p}_i$  represents momentum of the  $i$ th quark and  $\mathbf{p}_A$ ,  $\mathbf{p}_B$  and  $\mathbf{p}_C$  are the momentum of hadrons. In this work, the simple harmonic oscillator(SHO) wave function is chosen as the spatial part of the baryons[59],

$$\Psi(\mathbf{p}) = N \Psi_{n_\rho l_\rho m_{l_\rho}}(\mathbf{p}_\rho) \Psi_{n_\lambda l_\lambda m_{l_\lambda}}(\mathbf{p}_\lambda). \tag{6}$$

Here,  $N$  is a normalization coefficient of the wave function,  $\mathbf{p}_\rho$  and  $\mathbf{p}_\lambda$  represent the relative momentum between two light quarks, and between the heavy quark and the center of mass of two light quarks(Fig. 2), respectively. The relative wave function in the above equation is written as,

$$\Psi_{nlm_l}(\mathbf{p}) = (-1)^n (-i)^l R^{l+\frac{3}{2}} \sqrt{\frac{2n!}{\Gamma(n+l+\frac{3}{2})}} \exp\left(-\frac{R^2 \mathbf{p}^2}{2}\right) \times L_n^{l+1/2}(R^2 \mathbf{p}^2) |\mathbf{p}|^l Y_{lm_l}(\Omega_p), \tag{7}$$

where  $L_n^{l+1/2}(R^2 \mathbf{p}^2)$  is the Laguerre polynomial function, and  $Y_{lm_l}(\Omega_p)$  represents the spherical harmonic function. The relation between the solid harmonica polynomial  $y_{lm}(\mathbf{p})$  and  $Y_{lm_l}(\Omega_p)$  can be written as  $y_{lm}(\mathbf{p}) = |\mathbf{p}|^l Y_{lm_l}(\Omega_p)$ .

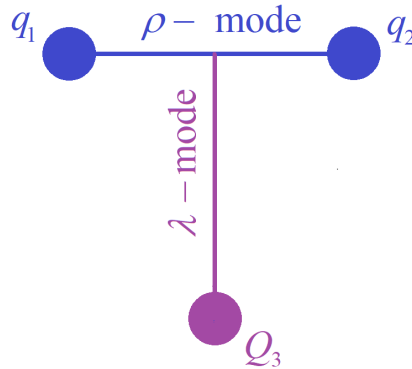


FIG. 2: The  $\rho$ - and  $\lambda$ -mode excitations in a single heavy baryon system.  $q_1$  and  $q_2$  denote the light  $u$ ,  $d$  and  $s$  quarks, and  $Q_3$  corresponds to a heavy charm or bottom quark.

In the heavy quark limit, the heavy quark in a single heavy baryon is decoupled from two light quarks. Under this picture, the dynamics of a single heavy baryon are commonly separated into two parts, which is illustrated in Fig. 2. The degree of freedom between two light quarks( $q_1$  and  $q_2$ ) is

called  $\rho$ -mode, while the degree of freedom between the center of mass of two light quarks and the heavy quark is called  $\lambda$ -mode. For  $P$ -wave baryons, there are two orbital excitation modes  $\lambda$ - and  $\rho$ -mode with  $(l_\rho, l_\lambda)=(0,1)$  and  $(1,0)$  respectively. While there are three excitation modes for  $D$ -wave baryons with  $(l_\rho, l_\lambda)=(0,2)$ ,  $(2,0)$  and  $(1,1)$ , which are called the  $\lambda$ -mode,  $\rho$ -mode and  $\lambda$ - $\rho$  mixing mode, respectively. It is indicated that the lowest state of a single heavy baryon is dominated by the  $\lambda$ -mode excitations and almost all experimentally observed single heavy baryons can be interpreted as  $\lambda$ -mode excited states[17, 49]. Thus, only the strong decays of single heavy baryons with  $\lambda$ -mode orbital excitations are considered in this work.

### 3 Numerical results and discussions

The final results of  ${}^3P_0$  model depend on some input parameters such as the quark pair ( $q\bar{q}$ ) creation strength  $\gamma$ , the SHO wave function scale parameter  $R$ , and the masses of the hadrons. As for the quark pair creation strength, we take the universal value  $\gamma = 13.4$ [22, 41, 46]. For the heavy baryons, the parameters  $R_{\lambda,\rho}$  can be fixed to reproduce the mass splitting through the contact term in the potential model[59]. Their values are taken as  $R_{\lambda,\rho} = 1.67 \text{ GeV}^{-1}$  for  $1S$ -wave baryon,  $R_{\lambda,\rho} = 2.0 \text{ GeV}^{-1}$  for  $P$ -wave baryon and  $R_{\lambda,\rho} = 2.5 \text{ GeV}^{-1}$  for  $2S$ - and  $2D$ -wave baryons[41, 46, 59]. As for the light mesons, the value of  $R$  was suggested to be  $2.5 \text{ GeV}^{-1}$  in Ref.[22–24], where it was determined by performing a series of least squares fits of the model predictions to the decay widths of 28 of the best known meson decays. For heavier mesons, their values are different from light meson's and are taken as  $R_B = 1.59 \text{ GeV}^{-1}$ ,  $R_{B_s} = 1.53 \text{ GeV}^{-1}$ ,  $R_D = 1.67 \text{ GeV}^{-1}$  and  $R_{D_s} = 1.63 \text{ GeV}^{-1}$ [60, 61]. All these  $R$  values of heavy mesons were predicted by the relativistic quark model[60, 61]. With the predicted masses in Refs.[17], we study the OZI-allowed strong decay behaviors of the  $1S$ ,  $2S$ ,  $1P$ ,  $2P$  states and some of the  $1D$ ,  $2D$  states. The results are presented in Tables IV–XXI of Appendix A. In these tables, the single heavy baryons are denoted as  $\Lambda_{Qj}^{L\lambda'(\rho')}$ ,  $\Sigma_{Qj}^{L\lambda'(\rho')}$  and  $\Omega_{Qj}^{L\lambda'(\rho')}$ , where the superscript  $L$  is the total orbital angular momentum with  $L = l_\rho + l_\lambda$ . The superscripts  $\lambda'$  and  $\rho'$  denote the first radial excitation with  $(n_\rho, n_\lambda)=(0, 1)$  and  $(1, 0)$ , respectively. The subscript  $j$  represents the total angular momentum of light quarks which satisfies  $j = L + S$ . The experimental information[62, 63] and predictions from quark model[17] for  $\Lambda_Q$ ,  $\Sigma_Q$  and  $\Omega_Q$  baryons are collected in I–III, and the predicted widths at present work by  ${}^3P_0$  model are also shown in the last column in these tables.

#### 3.1 $\Lambda_Q$ states

For  $\Lambda_Q$  systems, we can see from Tables I, IV–VII that the predicted decay widths are roughly compatible with the experimental data. For  $\Lambda_c(2765)$ , it was suggested as a  $2S(\frac{1}{2}^+)$  state by quark model[17]. The predicted total width of the  $2S$ -wave  $\Lambda_{c0}^{\lambda'}(\frac{1}{2}^+)$  state is 25.34 MeV(Table IV), which is lower than the experimental data. Considering the theoretical uncertainty, it is reasonable to assign  $\Lambda_c(2765)$  as the  $2S(\frac{1}{2}^+)$ . The theoretical total width for  $2P$ -wave  $\Lambda_{c1}^{\lambda'}(\frac{1}{2}^-)$  is 12.40 MeV(Table

IV), which is compatible with the experimental data of  $\Lambda_c(2940)$ . Thus,  $\Lambda_c(2940)$  can be assigned as the  $2P(\frac{1}{2}^-)$  state. As for the  $\Lambda_c(2860)$  and  $\Lambda_c(2880)$ , they were interpreted as a  $1D$  doublet ( $\frac{3}{2}^+, \frac{5}{2}^+$ ) by other collaborations[46]. Our predicted mass spectrum in quark model also supports this conclusion[17]. Under this assignment, the theoretical total width for  $\Lambda_c(2860)$  is 9.03 MeV (Tables I and V) which is consistent with the results of other collaborations[46]. However, this value is much lower than the experimental data which is about 67 MeV. We hope this divergence can be clarified in the future if more theoretical and experimental efforts were devoted into this problem.

TABLE I: Experimental information of  $\Lambda_Q(Q=c,b)$  baryons, and the predictions by quark model and  $^3P_0$  model. All values are in units of MeV

States	$J^P$	Experimental information[62, 63]			Quark model[17] $^3P_0$ model		
		Mass	Width	Decay channels	$J^P$	Mass	Width
$\Lambda_c^+$	$\frac{1}{2}^+$	2286.46±0.14	/	weak	$\frac{1}{2}^+(1S)$	2288	-
$\Lambda_c(2595)^+$	$\frac{1}{2}^-$	2592.25±0.28	2.59±0.30±0.47	$\Sigma_c^{++},^0\pi^{-,+}$	$\frac{1}{2}^-(1P)$	2596	11.44
$\Lambda_c(2625)^+$	$\frac{3}{2}^-$	2628.11±0.19	< 0.97	$\Sigma_c^{++},^0\pi^{-,+}$	$\frac{3}{2}^-(1P)$	2631	$1.0 \times 10^{-3}$
$\Lambda_c(2765)^+$	? <sup>?</sup>	2766.6±2.4	50	$\Sigma_c^{++}/^0\pi^\mp$	$\frac{1}{2}^+(2S)$	2764	25.34
$\Lambda_c(2860)^+$	$\frac{3}{2}^+$	2856.1 $_{-1.7}^{+2.0} \pm 0.5_{-5.6}^{+1.1}$	67.6 $_{-8.1}^{+10.1} \pm 1.4_{-20.0}^{+5.9}$	$D^0 p$	$\frac{3}{2}^+(1D)$	2875	9.03
$\Lambda_c(2880)^+$	$\frac{5}{2}^+$	2881.63±0.24	5.6 $_{-0.6}^{+0.8}$	$\Sigma_c^{(*)++},^0\pi^{-,+}, D^0 p$	$\frac{5}{2}^+(1D)$	2891	7.22
$\Lambda_c(2940)^+$	? <sup>?</sup>	2939.6 $_{-1.5}^{+1.3}$	20 $_{-6}^{+6}$	$\Sigma_c^{++},^0\pi^{-,+}$	$\frac{1}{2}^-(2P)$	2988	12.40
$\Lambda_b(6072)^0$	? <sup>?</sup>	6072.3±2.9	72±11	$\Lambda_b^0\pi^+\pi^-$	$\frac{1}{2}^+(2S)$	6041	8.82
$\Lambda_b(6146)^0$	$\frac{3}{2}^+$	6146.17±0.4	2.9±1.3	$\Lambda_b^0\pi^+\pi^-$	$\frac{3}{2}^+(1D)$	6137	5.99
$\Lambda_b(6152)^0$	$\frac{5}{2}^+$	6152.5±0.4	2.1±0.9	$\Lambda_b^0\pi^+\pi^-$	$\frac{5}{2}^+(1D)$	6145	5.43

The bottom baryons  $\Lambda_b(6072)$ ,  $\Lambda_b(6146)$  and  $\Lambda_b(6152)$  were observed in the  $\Lambda_b^0\pi^+\pi^-$  invariant mass spectrum. It is known that this three-body decay to  $\Lambda_b^0\pi^+\pi^-$  can take place according to intermediate  $\Sigma_b^\pm$  and  $\Sigma_b^{*\pm}$  states. For  $\Lambda_b(6152)$  as an example, the  $\Lambda_b(6152) \rightarrow \Sigma_b\pi$  and  $\Lambda_b(6152) \rightarrow \Sigma_b^*\pi$  processes have been clearly visible[13]. Thus, the two-body strong decay properties are commonly estimated by the  $^3P_0$  model, which serves as an important information to understand the nature of these newly observed baryons[47, 49, 51, 54, 64]. In many references,  $\Lambda_b(6146)$  and  $\Lambda_b(6152)$  were suggested to be the  $1D$ -wave doublet ( $\frac{3}{2}^+, \frac{5}{2}^+$ ) which are the partners of the  $\Lambda_c(2860)$  and  $\Lambda_c(2880)$ [49, 51]. In this work, the predicted total widths for this doublet are 5.99 MeV and 5.43 MeV (Tables I and VII), respectively. These values are comparable with the experimental measurements and consistent well with the predictions of other collaborations[49, 51]. However, the LHCb announced that they did not observe significant  $\Lambda_b(6146) \rightarrow \Sigma_b^\pm\pi^\pm$  signals in their experiments. This divergence between experiments and model prediction needs further confirmation.

As for  $\Lambda_b(6072)$ , the LHCb Collaboration suggested that it can be assigned as the first radial excitation of  $\Lambda_b$  baryon[12],  $2S(\frac{1}{2}^+)$  state. The predicted masses for the  $2S(\frac{1}{2}^+)$ ,  $1P(\frac{1}{2}^-)$  and  $1P(\frac{3}{2}^-)$

$\Lambda_b$  baryons by constituent quark model[17] are 6041 MeV, 5898 MeV and 5913 MeV, respectively. The measured mass of  $\Lambda_b(6072)$  is 6072 MeV[12], which is compatible with the prediction for  $2S(\frac{1}{2}^+)$  state from quark model. However, the theoretical width for  $2S(\frac{1}{2}^+)$  state is 8.82 MeV in this work(Tables I and VI), which is much smaller than the experimental data. In Ref.[64], the predicted width for  $2S(\frac{1}{2}^+)$  state was 9.27 MeV, which is also significantly smaller than experimental data and consistent with our results. In their studies, they also treated  $\Lambda_b(6072)$  as a 1P-wave state and predicted its total width to be 72 MeV by considering the mixing mechanism. However, the theoretical masses of 1P-wave  $\Lambda_b$  baryons[17] are not consistent with experiments. This divergence between theoretical prediction and experimental data suggests that the nature of  $\Lambda_b(6072)$  needs further verification by different theoretical methods and experiments.

It is also shown in Tables IV-VI, the predicted total widths for  $2P$ -wave states  $\Lambda_{c1}^{1\lambda'}(\frac{3}{2}^-)$ ,  $\Lambda_{b1}^{1\lambda'}(\frac{1}{2}^-)$  and  $\Lambda_{b1}^{1\lambda'}(\frac{3}{2}^-)$  are 13.31 MeV, 5.97 MeV and 5.81 MeV, respectively. These widths are relatively narrow, which indicates these states have good potentials to be discovered in the future. To be more specific, the main decay channels are  $\Sigma_c^{*+,0}\pi^{0,+}$ ,  $D^{*0}p$  and  $D^{*+}n$  for  $\Lambda_{c1}^{1\lambda'}(\frac{3}{2}^-)$ , while  $\Sigma_b^{+,0,-}\pi^{-,0,+}$  and  $\Sigma_b^{*+,0,-}\pi^{-,0,+}$  are the main decay modes for  $\Lambda_{b1}^{1\lambda'}(\frac{1}{2}^-)$  and  $\Lambda_{b1}^{1\lambda'}(\frac{3}{2}^-)$ , respectively.

### 3.2 $\Sigma_Q$ states

TABLE II: Experimental information of  $\Sigma_Q(Q=c,b)$  baryons, and the predictions by quark model and  ${}^3P_0$  model. All values are in units of MeV

States	Experimental information[62, 63]				Quark model[17]		${}^3P_0$ model
	$J^P$	Mass	Width	Decay channels	$J^P$	Mass	width
$\Sigma_c(2455)^{++}$	$\frac{1}{2}^+$	$2453.97\pm 0.14$	$1.89_{-0.18}^{+0.09}$	$\Lambda_c^+\pi$	$\frac{1}{2}^+(1S)$	2457	-
$\Sigma_c(2455)^+$	$\frac{1}{2}^+$	$2452.9\pm 0.4$	$<4.6$	$\Lambda_c^+\pi$			
$\Sigma_c(2455)^0$	$\frac{1}{2}^+$	$2453.75\pm 0.14$	$1.83_{-0.19}^{+0.11}$	$\Lambda_c^+\pi$			
$\Sigma_c(2520)^{++}$	$\frac{3}{2}^+$	$2518.41_{-0.19}^{+0.21}$	$14.78_{-0.40}^{+0.30}$	$\Lambda_c^+\pi$	$\frac{3}{2}^+(1S)$	2532	12.90
$\Sigma_c(2520)^+$	$\frac{3}{2}^+$	$2517.5\pm 2.3$	$<17$	$\Lambda_c^+\pi$			
$\Sigma_c(2520)^0$	$\frac{3}{2}^+$	$2518.48\pm 0.20$	$15.3_{-0.5}^{+0.4}$	$\Lambda_c^+\pi$			
$\Sigma_c(2800)^{++}$	$?^?$	$2801_{-6}^{+4}$	$75_{-17}^{+22}$	$\Lambda_c^+\pi$	$\frac{3}{2}^-(1P)$	2802	60~70
$\Sigma_c(2800)^+$	$?^?$	$2792_{-5}^{+14}$	$62_{-40}^{+60}$	$\Lambda_c^+\pi$			
$\Sigma_c(2800)^0$	$?^?$	$2806_{-7}^{+5}$	$72_{-15}^{+22}$	$\Lambda_c^+\pi$			
$\Sigma_b^-$	$\frac{1}{2}^+$	$5815.64\pm 0.27$	$5.3\pm 0.5$	$\Lambda_b^0\pi$	$\frac{1}{2}^+(1S)$	5820	-
$\Sigma_b^+$	$\frac{1}{2}^+$	$5810.56\pm 0.25$	$5.0\pm 0.5$	$\Lambda_b^0\pi$			
$\Sigma_b^{*+}$	$\frac{3}{2}^+$	$5830.32\pm 0.27$	$9.4\pm 0.5$	$\Lambda_b^0\pi$	$\frac{3}{2}^+(1S)$	5849	14.00
$\Sigma_b^{*-}$	$\frac{3}{2}^+$	$5834.74\pm 0.30$	$10.4\pm 0.8$	$\Lambda_b^0\pi$			
$\Sigma_b(6097)^-$	$?^?$	$6098.0\pm 1.8$	$29\pm 4$	$\Lambda_b\pi, \Sigma_b\pi, \Sigma_b^*\pi$	$\frac{3}{2}^-(1P)$	6104	30
$\Sigma_b(6097)^+$	$?^?$	$6095.8\pm 1.7$	$31\pm 6$	$\Lambda_b\pi, \Sigma_b\pi, \Sigma_b^*\pi$			

As for the  $\Sigma_Q$  baryons, the lowest  $S$ -wave states  $\frac{1}{2}^+$  and  $\frac{3}{2}^+$  have been observed and confirmed[62, 63]. However, the spin-parities of experimentally observed  $\Sigma_c(2800)$  and  $\Sigma_b(6097)$  need confirmation in more ways[45, 48]. According to the predictions by quark model, both  $\Sigma_c(2800)$  and  $\Sigma_b(6097)$  can be accommodated in the mass spectra as lowest-lying  $P$ -wave states. Yet it is noted that there are five  $1P$ -wave states in quark model, where their masses are close to each other[17]. The  $\Sigma_b(6097)$  is proposed to be a  $1P(\frac{3}{2}^-)_{j=2}$  state by quark model and so does  $\Sigma_c(2800)$ . From Tables VIII-XIII, we can see that both  $\Sigma_c(2800)$  and  $\Sigma_b(6097)$  are impossible the spin singlet  $J^P = \frac{1}{2}^-$  or the spin doublet  $(\frac{1}{2}^-, \frac{3}{2}^-)_{j=1}$  because of their large theoretical widths. For  $\Sigma_b$  baryons, the predicted total widths for  $\Sigma_{b2}^1(\frac{3}{2}^-)$  or  $\Sigma_{b2}^1(\frac{5}{2}^-)$  are 15.64 MeV and 18.65 MeV respectively(Table XIII), which are close to each other and at the same order of magnitude with the experimental data. Because the predicted mass for  $\Sigma_{b2}^1(\frac{3}{2}^-)$  by quark model is closer to the measured results[17], the  $\Sigma_{b2}^1(\frac{3}{2}^-)$  is a better candidate for  $\Sigma_b(6097)$ . As for  $\Sigma_c(2800)$ , its situation is very similar with that of  $\Sigma_b(6097)$ [65–67] and the possible assignment for it is  $\Sigma_{c2}^1(\frac{3}{2}^-)$ . If these assignments for  $\Sigma_c(2800)$  and  $\Sigma_b(6097)$  are true, their predicted total widths are still lower than measured values. Especially for  $\Sigma_c(2800)$ , its theoretical width is 19.13 MeV, which is much lower than experimental data. The first interpretation of this deviation is the uncertainties of the  $^3P_0$  model. In the following, we will see that the result from the  $^3P_0$  model may be a factor of  $2 \sim 3$  off the experimental width. Another interpretation of this problem is the mixing mechanism of the quark model states. We know that the physical resonances can be the mixing of the quark model states with the same  $J^P$ [68],

$$\begin{pmatrix} |1P\frac{1}{2}^-\rangle_1 \\ |1P\frac{1}{2}^-\rangle_2 \end{pmatrix} = \begin{pmatrix} \cos\theta & \sin\theta \\ -\sin\theta & \cos\theta \end{pmatrix} \begin{pmatrix} |\frac{1}{2}^-, j=0\rangle \\ |\frac{1}{2}^-, j=1\rangle \end{pmatrix}, \quad (8)$$

$$\begin{pmatrix} |1P\frac{3}{2}^-\rangle_1 \\ |1P\frac{3}{2}^-\rangle_2 \end{pmatrix} = \begin{pmatrix} \cos\theta & \sin\theta \\ -\sin\theta & \cos\theta \end{pmatrix} \begin{pmatrix} |\frac{3}{2}^-, j=1\rangle \\ |\frac{3}{2}^-, j=2\rangle \end{pmatrix}. \quad (9)$$

That is to say, state mixing can occur between  $|\frac{3}{2}^-, j=1\rangle$  and  $|\frac{3}{2}^-, j=2\rangle$  as in Eq.(9). Considering the mixing mechanism, we plot the total decay widths of the mixing states  $|1P\frac{3}{2}^-\rangle_1$  and  $|1P\frac{3}{2}^-\rangle_2$  versus the mixing angle  $\theta$  in the range  $0^\circ \sim 30^\circ$  in Figs. 3-4. When the mixing angle  $\theta$  is constrained in  $10^\circ \sim 15^\circ$  in Fig. 4, the total width of  $|1P\frac{3}{2}^-\rangle_2$  can reach about 30 MeV, which is consistent with the experimental data. Thus,  $\Sigma_b(6097)$  can be interpreted as a mixing state of  $|\frac{3}{2}^-, j=1\rangle$  and  $|\frac{3}{2}^-, j=2\rangle$ . It is same for  $\Sigma_c(2800)$ , if the mixing angle equals to  $30^\circ$  in Fig. 3, the total width of  $|1P\frac{3}{2}^-\rangle_2$  can reach 60 MeV $\sim$ 70 MeV, which indicates  $\Sigma_c(2800)$  is possibly a mixing state of  $|\frac{3}{2}^-, j=1\rangle$  and  $|\frac{3}{2}^-, j=2\rangle$ .

The theoretical widths of  $1P$ -wave  $\Sigma_c(\frac{5}{2}^-)$  and  $\Sigma_b(\frac{5}{2}^-)$  which are still missing in experiments, are predicted to be 22.42 MeV and 18.65 MeV, respectively(Tables X and XIII). It is shown that  $\Lambda_c\pi^+$  and  $\Lambda_b\pi^+$  are the ideal channels to search for these two states. As mentioned in Ref.[17], the  $2S$ -wave



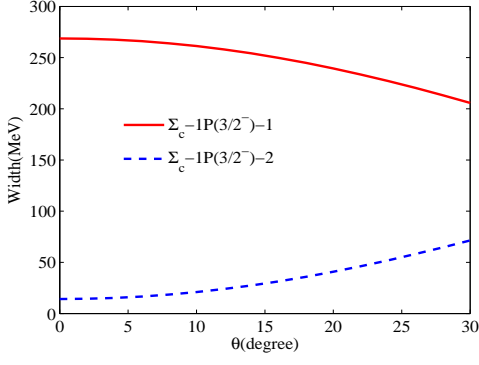


FIG. 3: The total decay widths of  $|1P_{\frac{3}{2}}^{-}\rangle_1$  and  $|1P_{\frac{3}{2}}^{-}\rangle_2$  for  $\Sigma_c$  as functions of the mixing angle  $\theta$  in the range  $0^\circ \sim 30^\circ$ .

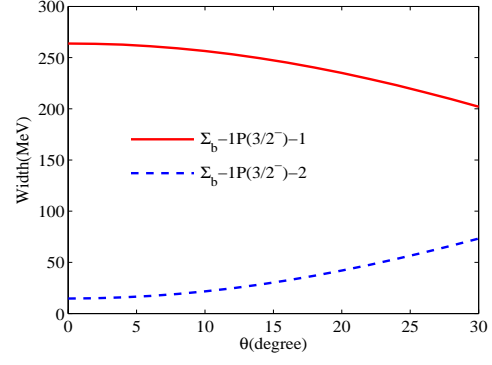


FIG. 4: The total decay widths of  $|1P_{\frac{3}{2}}^{-}\rangle_1$  and  $|1P_{\frac{3}{2}}^{-}\rangle_2$  for  $\Sigma_b$  as functions of the mixing angle  $\theta$  in the range  $0^\circ \sim 30^\circ$ .

$\Sigma_Q(\frac{1}{2}^+)$  and  $\Sigma_Q(\frac{3}{2}^+)$  are also expected to be observed in experiments. The theoretical widths for  $2S$  states  $\Sigma_{c1}^{0\rho'}(\frac{1}{2}^+)$ ,  $\Sigma_{c1}^{0\rho'}(\frac{3}{2}^+)$ ,  $\Sigma_{b1}^{0\rho'}(\frac{1}{2}^+)$ , and  $\Sigma_{b1}^{0\rho'}(\frac{3}{2}^+)$  are 11 ~ 13 MeV (Tables VIII and XI), which are relatively narrow. This implies that these states may easily be observed in future experiments. The decay modes  $\Sigma_c^{++,+}\pi^{0,+}$  and  $\Sigma_c^{*++,+}\pi^{0,+}$  provide dominating contributions to the total widths of  $\Sigma_{c1}^{0\rho'}(\frac{1}{2}^+)$  and  $\Sigma_{c1}^{0\rho'}(\frac{3}{2}^+)$ , while  $\Sigma_b^{+,0}\pi^{0,+}$ , and  $\Sigma_b^{*+,0}\pi^{0,+}$  are the dominating decay channels for  $\Sigma_{b1}^{0\rho'}(\frac{1}{2}^+)$  and  $\Sigma_{b1}^{0\rho'}(\frac{3}{2}^+)$  states.

### 3.3 $\Omega_Q$ states

As for the newly observed  $\Omega_c(3185)$  and  $\Omega_c(3327)$ , their masses are consistent with the predictions for  $2S(\frac{3}{2}^+)$  and  $1D$  states by quark model [17]. As a  $2S$ -wave  $\Omega_{c1}^{0\lambda'}(\frac{3}{2}^+)$  state, the theoretical width of  $\Omega_c(3185)$  is 78.16 MeV (Tables III and XIV). This value is close to the experimental data  $50 \pm 7_{-20}^{+10}$  MeV. Thus, it is reasonable to assign  $\Omega_c(3185)$  as a  $2S(\frac{3}{2}^+)$  state. The  $\Omega_c(3327)$  is discovered in the decay channel  $\Xi_c^+ K^-$  with a total width being  $20 \pm 5_{-1}^{+13}$  MeV [1]. From Table XVII, we can see the decay channels and total widths of  $1D$ -wave  $\frac{1}{2}^+$  and  $\frac{3}{2}^+$  states are both compatible with experimental data. However, the predicted mass for the latter, 3313 MeV [17], is closer to experiments. Therefore,  $\Omega_c(3327)$  is possibly a  $1D(\frac{3}{2}^+)$  state.

According to the mass spectrum [17], the previously observed baryons  $\Omega_c(3120)$ , ( $\Omega_c(3000)$ ,  $\Omega_c(3050)$ ) and ( $\Omega_c(3065)$ ,  $\Omega_c(3090)$ ) were suggested as a  $2S(\frac{1}{2}^+)$  state, the  $1P$  doublets  $(\frac{1}{2}^-, \frac{3}{2}^-)_{j=1}$  and  $(\frac{3}{2}^-, \frac{5}{2}^-)_{j=2}$ , respectively. As a  $2S$ -wave  $\Omega_{c1}^{0\rho'}(\frac{1}{2}^+)$  state, the theoretical width of  $\Omega_c(3120)$  is 5.95 MeV (Table XIV), which is slightly larger than the experimental data (Table III). Given the theoretical uncertainty, it is reasonable to interpret  $\Omega_c(3120)$  as a  $2S(\frac{1}{2}^+)$  state. This also means that  $\Omega_c(3120)$  and  $\Omega_c(3185)$  are a  $2S$  doublet  $(\frac{1}{2}^+, \frac{3}{2}^+)$ . It is shown in Tables XIV-XVI that the predicted widths for the five  $1P$ -wave states,  $\Omega_{c0}^1(\frac{1}{2}^-)$ ,  $\Omega_{c1}^1(\frac{1}{2}^-)$ ,  $\Omega_{c1}^1(\frac{3}{2}^-)$ ,  $\Omega_{c2}^1(\frac{3}{2}^-)$  and  $\Omega_{c2}^1(\frac{5}{2}^-)$  are 364 MeV,  $2.18 \times 10^{-11}$

TABLE III: Experimental information of  $\Omega_Q(Q=c,b)$  baryons, and the predictions by quark model and  ${}^3P_0$  model. All values are in units of MeV

States	$J^P$	Experimental information[62, 63]			Quark model[17]		${}^3P_0$ model
		Mass	Width	Decay channels	$J^P$	Mass	width
$\Omega_c^0$	$\frac{1}{2}^+$	$2695.2 \pm 1.7$	-	-	$\frac{1}{2}^+(1S)$	2699	-
$\Omega_c(2770)^0$	$\frac{3}{2}^+$	$2765.9 \pm 2.0$	-	-	$\frac{3}{2}^+(1S)$	2762	-
$\Omega_c(3000)^0$	??	$3000.4 \pm 0.2 \pm 0.1 \pm 0.3$	$4.5 \pm 0.6 \pm 0.3$	$\Xi_c^+ K^-$	$1P(\frac{1}{2}^-)_{j=1}$	3045	$4.00 \sim 5.00$
$\Omega_c(3050)^0$	??	$3050.2 \pm 0.1 \pm 0.1 \pm 0.3$	$< 1.2$	$\Xi_c^+ K^-$	$1P(\frac{3}{2}^-)_{j=1}$	3062	$< 1.00$
$\Omega_c(3065)^0$	??	$3065.6 \pm 0.1 \pm 0.3 \pm 0.3$	$3.5 \pm 0.4 \pm 0.2$	$\Xi_c^+ K^-$	$1P(\frac{3}{2}^-)_{j=2}$	3039	1.00
$\Omega_c(3090)^0$	??	$3090.2 \pm 0.3 \pm 0.5 \pm 0.3$	$8.7 \pm 1.0 \pm 0.8$	$\Xi_c^+ K^-$	$1P(\frac{5}{2}^-)_{j=2}$	3067	2.50
$\Omega_c(3120)^0$	??	$3119.1 \pm 0.3 \pm 0.9 \pm 0.3$	$< 2.6$	$\Xi_c^+ K^-$	$\frac{1}{2}^+(2S)$	3150	5.95
$\Omega_c(3185)^0$	??	$3185.1 \pm 1.7_{-0.9}^{+7.4} \pm 0.2$	$50 \pm 7_{-20}^{+10}$	$\Xi_c^+ K^-$	$\frac{3}{2}^+(2S)$	3197	78.16
$\Omega_c(3327)^0$	??	$3327.1 \pm 1.2_{-1.3}^{+0.1} \pm 0.2$	$20 \pm 5_{-1}^{+13}$	$\Xi_c^+ K^-$	$\frac{3}{2}^+(1D)$	3313	25.20
$\Omega_b(6316)^-$	??	$6315.64 \pm 0.31 \pm 0.07 \pm 0.50$	$< 2.8(4.2)$	$\Xi_b^0 K^-$	$1P(\frac{1}{2}^-)_{j=1}$	6329	$1.00 \sim 2.00$
$\Omega_b(6330)^-$	??	$6330.30 \pm 0.28 \pm 0.07 \pm 0.50$	$< 3.1(4.7)$	$\Xi_b^0 K^-$	$1P(\frac{3}{2}^-)_{j=1}$	6336	0.23
$\Omega_b(6340)^-$	??	$6339.71 \pm 0.26 \pm 0.05 \pm 0.50$	$< 1.5(1.8)$	$\Xi_b^0 K^-$	$1P(\frac{3}{2}^-)_{j=2}$	6326	0.05
$\Omega_b(6350)^-$	??	$6349.88 \pm 0.35 \pm 0.05 \pm 0.50$	$< 2.8(3.2)$	$\Xi_b^0 K^-$	$1P(\frac{5}{2}^-)_{j=2}$	6339	0.55

MeV,  $2.85 \times 10^{-10}$  MeV, 1.08 MeV and 2.50 MeV, respectively. In comparison with the experimental data, the assignments for  $\Omega_c(3065)$  and  $\Omega_c(3090)$  as a doublet  $(\frac{3}{2}^-, \frac{5}{2}^-)_{j=2}$  is reasonable. However, the predicted widths of the doublet  $(\frac{1}{2}^-, \frac{3}{2}^-)_{j=1}$  are very tiny, which means the above assignments for  $\Omega_c(3000)$  and  $\Omega_c(3050)$  is unreasonable. In Ref.[52], these two  $\Omega_c$  baryons were suggested to be the  $1D$ -wave states. However, the predicted masses in quark model for  $1D$ -wave  $\Omega_c$  are much larger than the experimental data, which indicates  $1D$ -wave states are not good candidates for  $\Omega_c(3000)$  and  $\Omega_c(3050)$ . Again, if we consider the mixing mechanism,  $\Omega_c(3000)$  and  $\Omega_c(3050)$  still can be described as the  $1P$ -wave states.

We plot the total widths of the mixing states versus the mixing angle  $\theta$  in the range  $0^\circ \sim 30^\circ$  in Figs. 5-6. It is shown that three mixing states  $|1P\frac{1}{2}^- \rangle_2$ ,  $|1P\frac{3}{2}^- \rangle_1$ , and  $|1P\frac{3}{2}^- \rangle_2$  belong to the narrow resonances. If the mixing angle  $\theta$  is constrained in a small value in Fig. 5, the total width of  $|1P\frac{1}{2}^- \rangle_2$  reaches 4~5 MeV. In addition, the values for  $|1P\frac{3}{2}^- \rangle_1$  and  $|1P\frac{3}{2}^- \rangle_2$  in Fig. 6 are all lower than 1 MeV. These results are roughly compatible with the experimental data. Thus, we tentatively assign the  $\Omega_c(3000)$ ,  $\Omega_c(3050)$ , and  $\Omega_c(3065)$  as the mixing states  $|1P\frac{1}{2}^- \rangle_2$ ,  $|1P\frac{3}{2}^- \rangle_1$  and  $|1P\frac{3}{2}^- \rangle_2$ , respectively and assign  $\Omega_c(3090)$  as a pure  $1P(\frac{5}{2}^-)$  state.

As for the narrow resonances,  $\Omega_b(6316)$ ,  $\Omega_b(6330)$ ,  $\Omega_b(6340)$ , and  $\Omega_b(6350)$ , their situation is very similar with the  $1P$ -wave  $\Omega_c$  states. After considering state mixing, the total width are plotted in Figs. 7-8. From these figures, we can obtain the similar conclusions with  $\Omega_c$  baryons, that  $\Omega_b(6316)$ ,

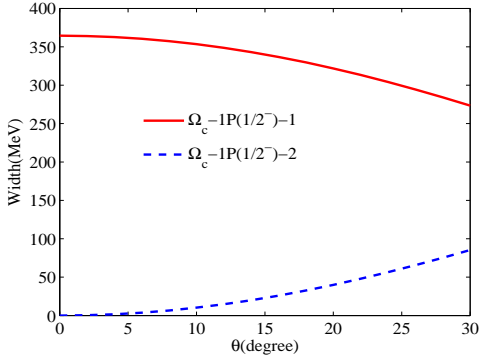


FIG. 5: The total decay widths of  $|1P_{\frac{1}{2}}^{-}\rangle_1$  and  $|1P_{\frac{1}{2}}^{-}\rangle_2$  for  $\Omega_c$  as functions of the mixing angle  $\theta$  in the range  $0^\circ \sim 30^\circ$ .

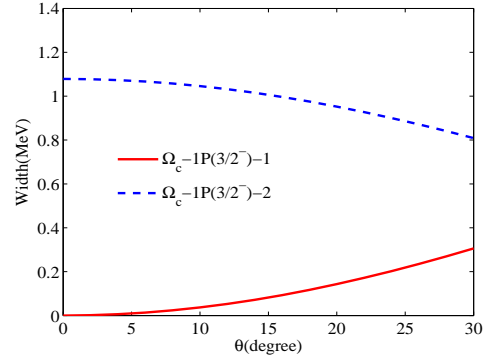


FIG. 6: The total decay widths of  $|1P_{\frac{3}{2}}^{-}\rangle_1$  and  $|1P_{\frac{3}{2}}^{-}\rangle_2$  for  $\Omega_c$  as functions of the mixing angle  $\theta$  in the range  $0^\circ \sim 30^\circ$ .

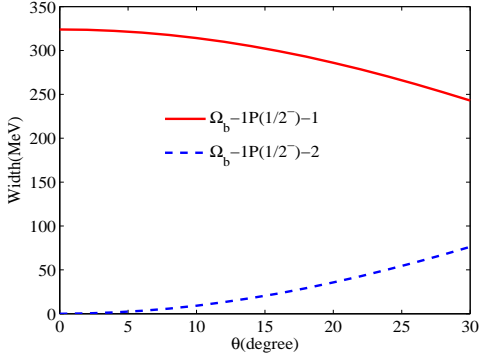


FIG. 7: The total decay widths of  $|1P_{\frac{1}{2}}^{-}\rangle_1$  and  $|1P_{\frac{1}{2}}^{-}\rangle_2$  for  $\Omega_b$  as functions of the mixing angle  $\theta$  in the range  $0^\circ \sim 30^\circ$ .

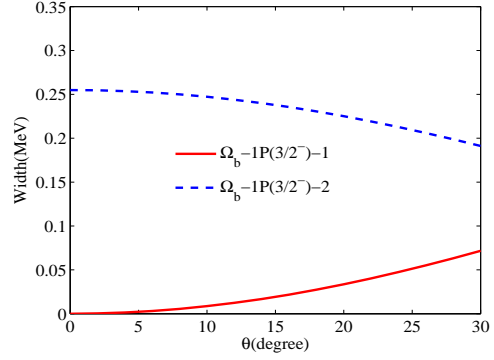


FIG. 8: The total decay widths of  $|1P_{\frac{3}{2}}^{-}\rangle_1$  and  $|1P_{\frac{3}{2}}^{-}\rangle_2$  for  $\Omega_b$  as functions of the mixing angle  $\theta$  in the range  $0^\circ \sim 30^\circ$ .

$\Omega_b(6330)$ ,  $\Omega_b(6340)$ , and  $\Omega_b(6350)$  can be respectively described as three mixing states  $|1P_{\frac{1}{2}}^{-}\rangle_2$ ,  $|1P_{\frac{3}{2}}^{-}\rangle_1$ ,  $|1P_{\frac{3}{2}}^{-}\rangle_2$ , and a pure state  $1P(\frac{5}{2}^-)$ . In Refs. [55, 68], they also obtained the same conclusions with ours.

Up to now, the  $2S$   $\Omega_c$  doublet  $(\frac{1}{2}^+, \frac{3}{2}^+)$  have been observed. However, their  $\Omega_b$  partners  $\Omega_b(\frac{1}{2}^+)$  and  $\Omega_b(\frac{3}{2}^+)$  are still missing in experiments. The results in Table XVIII show that the radial excited mode of these two states may be the  $\rho'$  excitations with  $(n_\rho, n_\lambda)=(1, 0)$ . Theoretical widths for these two states are 5.06 MeV and 4.63 MeV, respectively. They have the similar decay behaviors, both of them dominantly decay into  $\Xi_b^0 K^-$  and  $\Xi_b^- K^0$ .

As for the uncertainties of  $^3P_0$  model, it arise from the quark pair creation strength  $\gamma$ , the masses of hadrons, and the SHO wave function parameter  $R$ . The parameter of  $\gamma$  describes the strength of

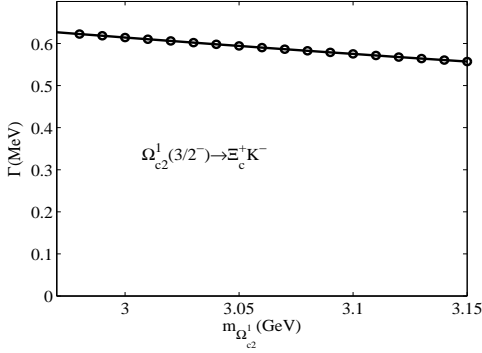


FIG. 9: The variation of the decay width of  $\Omega_{c2}^1(\frac{3}{2}^-) \rightarrow \Xi_c^+ K^-$  with the mass of  $\Omega_{c2}^1(\frac{3}{2}^-)$ .

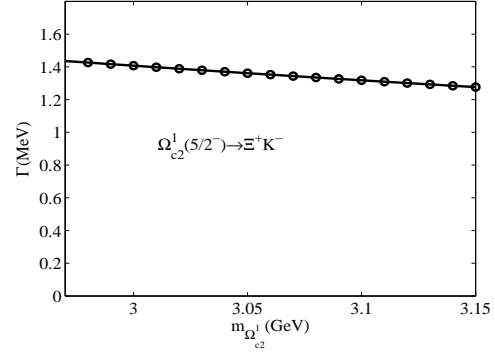


FIG. 10: The variation of the decay width of  $\Omega_{c2}^1(\frac{5}{2}^-) \rightarrow \Xi_c^+ K^-$  with the mass of  $\Omega_{c2}^1(\frac{5}{2}^-)$ .

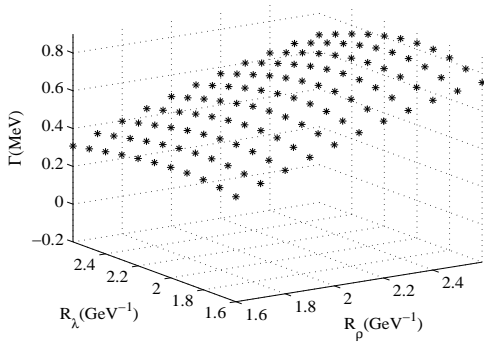


FIG. 11: The variation of the decay width of  $\Omega_{c2}^1(\frac{3}{2}^-) \rightarrow \Xi_c^+ K^-$  with  $R_\rho$  and  $R_\lambda$ .

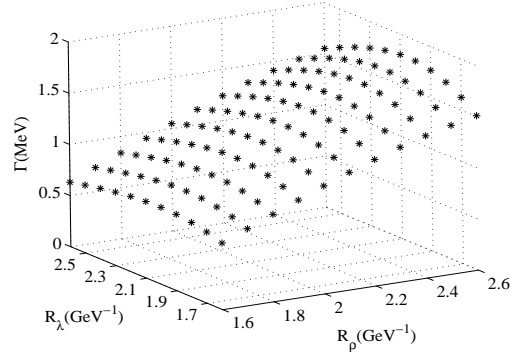


FIG. 12: The variation of the decay width of  $\Omega_{c2}^1(\frac{5}{2}^-) \rightarrow \Xi_c^+ K^-$  with  $R_\rho$  and  $R_\lambda$ .

quark-antiquark pair creation from the vacuum, and it is usually taken as the universal value of 13.4 which is fitted according to experimental data[22, 41, 46]. As for the masses of hadrons and scale parameters  $R$ , we illustrate the dependence of the results on them in Figs. 9-12, using two typical decay channels  $\Omega_{c2}^1(\frac{3}{2}^-) \rightarrow \Xi_c^+ K^-$  and  $\Omega_{c2}^1(\frac{5}{2}^-) \rightarrow \Xi_c^+ K^-$ . It is shown in Figs. 9-10 that the masses of initial heavy baryons have limited influence on the results. However, the predicted width changes 2 ~ 3 times when the parameters  $R_\rho$  and  $R_\lambda$  of  $\Omega_{c2}^1$  states change from 1.6  $\text{GeV}^{-1}$  to 2.6  $\text{GeV}^{-1}$  (Figs. 11-12). This indicates that the uncertainties mainly originate from parameters  $R$ . As discussed at the beginning of Section 3, we carefully take their values which are either fixed by fitting experimental data[22-24] or determined by solving the Schrödinger equation[41, 46, 59-61]. It is difficult to calculate the exact uncertainties of results originated from  $R$  because the uncertainties of  $R$  is unknown. It was stated in Ref. [41] that the maximum deviation of theoretical results may be a factor of 2 ~ 3 off the experimental width. Even with the above uncertainty, the  $^3P_0$  model is still the most systematic,

effective, and widely used framework to study the baryon strong decays. More detailed analysis about the uncertainties of the results in the  ${}^3P_0$  decay model can be found in Refs. [22, 41].

## 4 Conclusions

In this work, we have systematically investigated strong decay behaviors of the single heavy baryons  $\Lambda_Q$ ,  $\Sigma_Q$ , and  $\Omega_Q$ . A number of experimental states without spin-parity assignments are successfully distinguished. For example, the  $\Lambda_c(2940)$ ,  $\Lambda_c(2860)$ ,  $\Lambda_c(2880)$ ,  $\Lambda_b(6070)$  are suggested to be the  $2P(\frac{1}{2}^-)$ ,  $1D(\frac{1}{2}^+)$ ,  $1D(\frac{3}{2}^+)$  and  $2S(\frac{1}{2}^+)$  states, respectively. The  $\Sigma_c(2800)$  and  $\Sigma_b(6097)$  may be the pure quark model state  $1P(\frac{3}{2}^-)_{j=2}$ . Another possible interpretation is that each of them is the mixing state of  $|\frac{3}{2}^-, j=1\rangle$  and  $|\frac{3}{2}^-, j=2\rangle$ . The  $\Omega_c(3120)$  and  $\Omega_c(3185)$  are supported as the 2S doublet  $(\frac{1}{2}^+, \frac{3}{2}^+)$  and  $\Omega_c(3090)$  is assigned as the pure quark model state  $1P(\frac{5}{2}^-)$ . Model predictions support assigning the recently observed  $\Omega_c(3327)$  as a  $1D(\frac{3}{2}^+)$  state. As for  $\Omega_c(3000)$ ,  $\Omega_c(3050)$  and  $\Omega_c(3065)$ , they can be interpreted as the mixing states  $|1P\frac{1}{2}^- \rangle_2$ ,  $|1P\frac{3}{2}^- \rangle_1$ , and  $|1P\frac{3}{2}^- \rangle_2$ , respectively. The  $\Omega_b(6316)$ ,  $\Omega_b(6330)$ ,  $\Omega_b(6340)$ , and  $\Omega_b(6350)$  can be described as the mixing states  $|1P\frac{1}{2}^- \rangle_2$ ,  $|1P\frac{3}{2}^- \rangle_1$ ,  $|1P\frac{3}{2}^- \rangle_2$ , and a pure quark model state  $1P(\frac{5}{2}^-)$ , respectively.

A number of single heavy barons which have good potentials to be discovered in forthcoming experiments are predicted and some valuable clues for searching for these missing baryons are suggested by  ${}^3P_0$  decay model. For  $\Lambda_Q$  systems, we suggest to search for the  $2P$ -wave state  $\Lambda_{c1}^{1\lambda'}(\frac{3}{2}^-)$  in the decay channels  $\Sigma_c^{*+,0}\pi^{0,+}$ ,  $D^{*0}p$  and  $D^{*+}n$ . For  $\Lambda_b$  spin-doublet  $(\frac{1}{2}^-, \frac{3}{2}^-)_{j=1}$ , they are most likely to be found in decay channels  $\Sigma_b^{+,0,-}\pi^{-,0,+}$  and  $\Sigma_b^{*+,0,-}\pi^{-,0,+}$ , respectively. As mentioned in Section 3.1,  $\Lambda_c\pi^+$  and  $\Lambda_b\pi^+$  are the ideal decay channels to find the  $1P$ -wave  $\Sigma_c(\frac{5}{2}^-)$  and  $\Sigma_b(\frac{5}{2}^-)$  states. The  $2S$ -wave  $\Sigma_{c1}^{0\rho'}(\frac{1}{2}^+)$  and  $\Sigma_{c1}^{0\rho'}(\frac{3}{2}^+)$  have good potentials to be observed in the  $\Sigma_c^{++,+}\pi^{0,+}$  and  $\Sigma_c^{*++,+}\pi^{0,+}$  decay channels, while  $\Sigma_b^{+,0}\pi^{0,+}$ , and  $\Sigma_b^{*+,0}\pi^{0,+}$  are the dominating decay modes for  $\Sigma_{b1}^{0\rho'}(\frac{1}{2}^+)$  and  $\Sigma_{b1}^{0\rho'}(\frac{3}{2}^+)$  states. Finally, we suggest to hunt for the  $2S$ -wave doublet  $\Omega_b(\frac{1}{2}^+, \frac{3}{2}^+)$  in the  $\Xi_b^0 K^-$  and  $\Xi_b^- K^0$  decay channels.

## Acknowledgments

We would like to thank Si-Qiang Luo and Xiang Liu for their valuable discussions. This project is supported by the Natural Science Foundation of HeBei Province, Grant Number A2018502124.

- 
- [1] [LHCb], [arXiv:2302.04733](https://arxiv.org/abs/2302.04733) [hep-ex](2023).
  - [2] R. Aaij *et al.* [LHCb], *Phys. Rev. Lett.* **118**, no.18, 182001 (2017).
  - [3] H. Albrecht *et al.* [ARGUS], *Phys. Lett. B* **402**, 207-212 (1997).
  - [4] H. Albrecht *et al.* [ARGUS], *Phys. Lett. B* **317**, 227-232 (1993).
  - [5] P. L. Frabetti *et al.* [E687], *Phys. Rev. Lett.* **72**, 961-964 (1994).
  - [6] K. Tanida *et al.* [Belle], [arXiv:1908.06235](https://arxiv.org/abs/1908.06235) [hep-ex] (2019).

- [7] B. Aubert *et al.* [BaBar], *Phys. Rev. Lett.* **98**, 012001 (2007).
- [8] K. Abe *et al.* [Belle], *Phys. Rev. Lett.* **98**, 262001 (2007).
- [9] R. Aaij *et al.* [LHCb], *JHEP* **05**, 030 (2017).
- [10] R. Aaij *et al.* [LHCb], *Phys. Rev. Lett.* **109**, 172003 (2012).
- [11] T. A. Aaltonen *et al.* [CDF], *Phys. Rev. D* **88**, no.7, 071101 (2013).
- [12] R. Aaij *et al.* [LHCb], *JHEP* **06**, 136 (2020).
- [13] R. Aaij *et al.* [LHCb], *Phys. Rev. Lett.* **123**, no.15, 152001 (2019).
- [14] R. Mizuk *et al.* [Belle], *Phys. Rev. Lett.* **94**, 122002 (2005).
- [15] R. Aaij *et al.* [LHCb], *Phys. Rev. Lett.* **122**, no.1, 012001 (2019).
- [16] R. Aaij *et al.* [LHCb], *Phys. Rev. Lett.* **124**, no.8, 082002 (2020).
- [17] G. L. Yu, Z. Y. Li, Z. G. Wang, J. Lu and M. Yan, *Nucl. Phys. B* **990**, 116183 (2023).
- [18] L. Micu, *Nucl. Phys. B* **10**, 521-526 (1969).
- [19] A. Le Yaouanc, L. Oliver, O. Pene and J. C. Raynal, *Phys. Rev. D* **8**, 2223-2234 (1973); *Phys. Rev. D* **9**, 1415-1419 (1974); *Phys. Rev. D* **11**, 1272 (1975).
- [20] A. Le Yaouanc, L. Oliver, O. Pene and J. C. Raynal, *Phys. Lett. B* **71**, 397-399 (1977); *Phys. Lett. B* **72**, 57-61 (1977).
- [21] A. Le Yaouanc, L. Oliver, O. Pene and J. C. Raynal, *Hadron Transitions in the Quark Model* (Gordon and Breach Science Publishers, New York, 1987).
- [22] H. G. Blundell, [hep-ph/9608473](#) [hep-ph].
- [23] H. G. Blundell and S. Godfrey, *Phys. Rev. D* **53**, 3700-3711 (1996).
- [24] H. G. Blundell, S. Godfrey and B. Phelps, *Phys. Rev. D* **53**, 3712-3722 (1996).
- [25] E. S. Ackleh, T. Barnes and E. S. Swanson, *Phys. Rev. D* **54**, 6811-6829 (1996).
- [26] T. Barnes, N. Black and P. R. Page, *Phys. Rev. D* **68**, 054014 (2003).
- [27] F. E. Close and E. S. Swanson, *Phys. Rev. D* **72**, 094004 (2005).
- [28] F. E. Close, C. E. Thomas, O. Lakhina and E. S. Swanson, *Phys. Lett. B* **647**, 159-163 (2007).
- [29] H. Q. Zhou, R. G. Ping and B. S. Zou, *Phys. Lett. B* **611**, 123-128 (2005).
- [30] G. J. Ding and M. L. Yan, *Phys. Lett. B* **657**, 49-54 (2007).
- [31] B. Chen, D. X. Wang and A. Zhang, *Phys. Rev. D* **80**, 071502 (2009).
- [32] D. M. Li and S. Zhou, *Phys. Rev. D* **78**, 054013 (2008);
- [33] D. M. Li, P. F. Ji and B. Ma, *Eur. Phys. J. C* **71**, 1582 (2011).
- [34] D. M. Li and B. Ma, *Phys. Rev. D* **81**, 014021 (2010).
- [35] B. Zhang, X. Liu, W. Z. Deng and S. L. Zhu, *Eur. Phys. J. C* **50**, 617-628 (2007).
- [36] Y. Sun, Q. T. Song, D. Y. Chen, X. Liu and S. L. Zhu, *Phys. Rev. D* **89**, no.5, 054026 (2014).
- [37] Y. C. Yang, Z. Xia and J. Ping, *Phys. Rev. D* **81**, 094003 (2010).
- [38] G. L. Yu, Z. G. Wang and Z. Y. Li, *Phys. Rev. D* **94**, no.7, 074024 (2016).
- [39] G. L. Yu, Z. G. Wang and Z. Y. Li, *Chin. Phys. C* **39**, no.6, 063101 (2015); *Chin. Phys. C* **42**, no.4, 043107 (2018).
- [40] G. L. Yu and Z. G. Wang, *Chin. Phys. C* **44**, no.3, 033103 (2020).
- [41] C. Chen, X. L. Chen, X. Liu, W. Z. Deng and S. L. Zhu, *Phys. Rev. D* **75**, 094017 (2007).
- [42] D. D. Ye, Z. Zhao and A. Zhang, *Phys. Rev. D* **96**, no.11, 114009 (2017).

- [43] D. D. Ye, Z. Zhao and A. Zhang, *Phys. Rev. D* **96**, no.11, 114003 (2017).
- [44] B. Chen, X. Liu and A. Zhang, *Phys. Rev. D* **95**, no.7, 074022 (2017).
- [45] P. Yang, J. J. Guo and A. Zhang, *Phys. Rev. D* **99**, no.3, 034018 (2019).
- [46] J. J. Guo, P. Yang and A. Zhang, *Phys. Rev. D* **100**, no.1, 014001 (2019).
- [47] Q. F. Lü and X. H. Zhong, *Phys. Rev. D* **101**, no.1, 014017 (2020).
- [48] K. L. Wang, Q. F. Lü and X. H. Zhong, *Phys. Rev. D* **99**, no.1, 014011 (2019).
- [49] B. Chen, S. Q. Luo, X. Liu and T. Matsuki, *Phys. Rev. D* **100**, no.9, 094032 (2019).
- [50] Q. F. Lü, L. Y. Xiao, Z. Y. Wang and X. H. Zhong, *Eur. Phys. J. C* **78**, no.7, 599 (2018).
- [51] W. Liang, Q. F. Lü and X. H. Zhong, *Phys. Rev. D* **100**, no.5, 054013 (2019).
- [52] Z. Zhao, D. D. Ye and A. Zhang, *Phys. Rev. D* **95**, no.11, 114024 (2017).
- [53] Y. X. Yao, K. L. Wang and X. H. Zhong, *Phys. Rev. D* **98**, no.7, 076015 (2018).
- [54] K. L. Wang, Q. F. Lü and X. H. Zhong, *Phys. Rev. D* **100**, no.11, 114035 (2019).
- [55] L. Y. Xiao, K. L. Wang, M. S. Liu and X. H. Zhong, *Eur. Phys. J. C* **80**, no.3, 279 (2020).
- [56] L. Y. Xiao and X. H. Zhong, *Phys. Rev. D* **102**, no.1, 014009 (2020).
- [57] S. Q. Luo and X. Liu, [arXiv:2303.04022](https://arxiv.org/abs/2303.04022) [hep-ph].
- [58] X. Liu, H. W. Ke, X. Liu and X. Q. Li, *Eur. Phys. J. C* **76**, no.10, 549 (2016).
- [59] S. Capstick and N. Isgur, *Phys. Rev. D* **34**, no.9, 2809-2835 (1986).
- [60] S. Godfrey and K. Moats, *Phys. Rev. D* **93**, no.3, 034035 (2016).
- [61] S. Godfrey, K. Moats and E. S. Swanson, *Phys. Rev. D* **94**, no.5, 054025 (2016).
- [62] K. Nakamura *et al.* [Particle Data Group], *J. Phys. G* **37**, 075021 (2010).
- [63] P. A. Zyla *et al.* (Particle Data Group), *Prog. Theor. Exp. Phys.* 2020, 083C01 (2020).
- [64] W. Liang and Q. F. Lü, *Eur. Phys. J. C* **80**, no.8, 690 (2020).
- [65] H. M. Yang and H. X. Chen, *Phys. Rev. D* **104**, no.3, 034037 (2021).
- [66] K. L. Wang, Y. X. Yao, X. H. Zhong and Q. Zhao, *Phys. Rev. D* **96**, no.11, 116016 (2017).
- [67] H. X. Chen, Q. Mao, W. Chen, A. Hosaka, X. Liu and S. L. Zhu, *Phys. Rev. D* **95**, no.9, 094008 (2017).
- [68] W. Liang and Q. F. Lü, *Eur. Phys. J. C* **80**, no.3, 198 (2020).

## Appendix A: Two-body strong decays of $\Lambda_Q$ , $\Sigma_Q$ and $\Omega_Q$

TABLE IV: Two-body strong decays of  $\Lambda_c$  in MeV

N	1	2	3	4	5	6	7
Notations	$\Lambda_{c0}^{0\lambda'}$	$\Lambda_{c0}^{0\rho'}$	$\Lambda_{c1}^1$	$\Lambda_{c1}^{1\lambda'}$	$\Lambda_{c1}^{1\rho'}$	$\Lambda_{c1}^1$	$\Lambda_{c1}^{1\lambda'}$
Assignments	$\frac{1}{2}^+$ (2S)	$\frac{1}{2}^+$ (2S)	$\frac{1}{2}^-$ (1P)	$\frac{1}{2}^-$ (2P)	$\frac{1}{2}^-$ (2P)	$\frac{3}{2}^-$ (1P)	$\frac{3}{2}^-$ (2P)
Mass	2764	2764	2592	2988	2988	2628	3013
$\Sigma_c^{++}\pi^-$	5.04	1.49	2.72	2.34	6.84	$3.09\times 10^{-3}$	$8.50\times 10^{-2}$
$\Sigma_c^+\pi^0$	5.14	1.50	6.00	2.34	6.77	$3.93\times 10^{-3}$	$8.70\times 10^{-2}$
$\Sigma_c^0\pi^+$	5.04	1.49	2.72	2.34	6.84	$3.09\times 10^{-3}$	$8.50\times 10^{-2}$
$\Sigma_c^{*++}\pi^-$	3.33	1.26	-	$5.20\times 10^{-2}$	5.74	-	2.17
$\Sigma_c^{*+}\pi^0$	3.46	1.30	-	$5.70\times 10^{-2}$	5.80	-	2.17
$\Sigma_c^{*0}\pi^+$	3.33	1.26	-	0.052	5.74	-	2.17
$D^{*0}p$	-	-	-	2.67	2.81	-	3.31
$D^{*+}n$	-	-	-	2.55	2.80	-	3.23
$\Gamma_{total}$	25.34	8.30	11.44	12.40	43.34	$1.00\times 10^{-3}$	13.31

TABLE V: Two-body strong decays of  $\Lambda_c$  in MeV

N	1	2	3	4	5	6	7
Notations	$\Lambda_{c1}^{1\rho'}$	$\Lambda_{c2}^2$	$\Lambda_{c2}^{2\lambda'}$	$\Lambda_{c2}^{2\rho'}$	$\Lambda_{c2}^2$	$\Lambda_{c2}^{2\lambda'}$	$\Lambda_{c2}^{2\rho'}$
Assignments	$\frac{3}{2}^-$ (2P)	$\frac{3}{2}^+$ (1D)	$\frac{3}{2}^+$ (2D)	$\frac{3}{2}^+$ (2D)	$\frac{5}{2}^+$ (1D)	$\frac{5}{2}^+$ (2D)	$\frac{5}{2}^+$ (2D)
Mass	3013	2856	3220	3220	2882	3234	3234
$\Sigma_c^{++}\pi^-$	6.47	2.69	3.10	$8.90\times 10^{-2}$	$5.60\times 10^{-2}$	$8.40\times 10^{-1}$	$7.47\times 10^{-1}$
$\Sigma_c^+\pi^0$	6.51	2.71	3.11	$8.70\times 10^{-2}$	$5.70\times 10^{-2}$	$8.43\times 10^{-1}$	$7.50\times 10^{-1}$
$\Sigma_c^0\pi^+$	6.47	2.69	3.10	$8.90\times 10^{-2}$	$5.60\times 10^{-2}$	$8.39\times 10^{-1}$	$7.47\times 10^{-1}$
$\Sigma_c^{*++}\pi^-$	12.4	0.313	1.36	$8.98\times 10^{-1}$	2.34	3.93	$6.53\times 10^{-1}$
$\Sigma_c^{*+}\pi^0$	12.4	0.318	1.37	$9.01\times 10^{-2}$	2.37	3.93	$6.52\times 10^{-1}$
$\Sigma_c^{*0}\pi^+$	12.4	0.313	1.36	$8.98\times 10^{-2}$	2.34	3.93	$6.53\times 10^{-1}$
$\Lambda_c\omega$	-	-	2.53	2.57	-	2.81	2.70
$\Xi_c'^+K^0$	-	-	$1.58\times 10^{-1}$	$7.50\times 10^{-2}$	-	$2.67\times 10^{-3}$	$4.84\times 10^{-3}$
$\Xi_c'^0K^+$	-	-	$1.58\times 10^{-1}$	$7.50\times 10^{-2}$	-	$2.67\times 10^{-3}$	$4.84\times 10^{-3}$
$D^{*0}p$	2.69	-	2.90	$1.37\times 10^{-1}$	-	3.04	$1.66\times 10^{-1}$
$D^{*+}n$	2.73	-	2.87	$1.30\times 10^{-1}$	-	3.00	$1.58\times 10^{-1}$
$\Xi_c'^{*+}K^0$	-	-	$1.30\times 10^{-2}$	$8.84\times 10^{-3}$	-	$9.90\times 10^{-2}$	$6.00\times 10^{-2}$
$\Xi_c'^{*0}K^+$	-	-	$1.30\times 10^{-2}$	$8.84\times 10^{-3}$	-	$9.90\times 10^{-2}$	$6.00\times 10^{-2}$
$\Gamma_{total}$	62.07	9.03	22.04	5.97	7.22	23.37	7.36



TABLE VI: Two-body strong decays of  $\Lambda_b$  in MeV

N	1	2	3	4	5	6
Notations	$\Lambda_{b0}^{1\lambda'}$	$\Lambda_{b0}^{1\rho'}$	$\Lambda_{b1}^{1\lambda'}$	$\Lambda_{b1}^{1\rho'}$	$\Lambda_{b1}^{1\lambda'}$	$\Lambda_{b1}^{1\rho'}$
Assignments	$\frac{1}{2}^+$ (2S)	$\frac{1}{2}^+$ (2S)	$\frac{1}{2}^-$ (2P)	$\frac{1}{2}^-$ (2P)	$\frac{3}{2}^-$ (2P)	$\frac{3}{2}^-$ (2P)
Mass	6072	6072	6238	6238	6249	6249
$\Sigma_b^+ \pi^-$	1.39	$5.50 \times 10^{-1}$	1.98	11.5	$2.40 \times 10^{-2}$	2.76
$\Sigma_b^0 \pi^0$	1.39	$5.40 \times 10^{-1}$	1.97	11.5	$2.40 \times 10^{-2}$	2.73
$\Sigma_b^- \pi^+$	1.23	$4.90 \times 10^{-1}$	1.94	11.7	$2.20 \times 10^{-2}$	2.60
$\Sigma_b^{*+} \pi^-$	1.68	$7.00 \times 10^{-1}$	$2.80 \times 10^{-2}$	3.76	1.93	14.0
$\Sigma_b^{*0} \pi^0$	1.69	$7.00 \times 10^{-1}$	$2.80 \times 10^{-2}$	3.71	1.92	14.0
$\Sigma_b^{*-} \pi^+$	1.44	$6.10 \times 10^{-1}$	$2.60 \times 10^{-2}$	3.51	1.89	14.0
$\Gamma_{total}$	8.82	3.59	5.97	45.68	5.81	50.09

TABLE VII: Two-body strong decays of  $\Lambda_b$  in MeV

N	1	2	3	4	5	6
Notations	$\Lambda_{b2}^2$	$\Lambda_{b2}^{2\lambda'}$	$\Lambda_{b2}^{2\rho'}$	$\Lambda_{b2}^2$	$\Lambda_{b2}^{2\lambda'}$	$\Lambda_{b2}^{2\rho'}$
Assignments	$\frac{3}{2}^+$ (1D)	$\frac{3}{2}^+$ (2D)	$\frac{3}{2}^+$ (2D)	$\frac{5}{2}^+$ (1D)	$\frac{5}{2}^+$ (2D)	$\frac{5}{2}^+$ (2D)
Mass	6146	6432	6432	6153	6440	6440
$\Sigma_b^+ \pi^-$	1.75	2.95	$3.70 \times 10^{-1}$	$1.30 \times 10^{-2}$	$3.50 \times 10^{-1}$	$4.20 \times 10^{-1}$
$\Sigma_b^0 \pi^0$	1.74	2.94	$3.80 \times 10^{-1}$	$1.30 \times 10^{-2}$	$3.50 \times 10^{-1}$	$4.10 \times 10^{-1}$
$\Sigma_b^- \pi^+$	1.65	2.91	$3.90 \times 10^{-1}$	$1.10 \times 10^{-2}$	$3.30 \times 10^{-1}$	$4.00 \times 10^{-1}$
$\Sigma_b^{*+} \pi^-$	$2.90 \times 10^{-1}$	1.02	$6.70 \times 10^{-1}$	1.84	3.67	$7.60 \times 10^{-1}$
$\Sigma_b^{*0} \pi^0$	$2.90 \times 10^{-1}$	1.01	$6.60 \times 10^{-1}$	1.82	3.65	$7.60 \times 10^{-1}$
$\Sigma_b^{*-} \pi^+$	$2.70 \times 10^{-1}$	0.99	$6.40 \times 10^{-1}$	1.73	3.60	$7.70 \times 10^{-1}$
$\Lambda_b \omega$	-	$4.50 \times 10^{-1}$	$5.30 \times 10^{-1}$	-	$6.40 \times 10^{-1}$	$7.20 \times 10^{-1}$
$B^{*-} p$	-	2.72	$8.80 \times 10^{-2}$	-	2.85	$1.10 \times 10^{-1}$
$B^{*0} n$	-	2.71	$8.70 \times 10^{-2}$	-	2.84	$1.10 \times 10^{-1}$
$\Gamma_{total}$	5.99	17.7	3.82	5.43	18.28	4.46

TABLE VIII: Two-body strong decays of  $\Sigma_c$  in MeV

N	1	2	3	4	5	6	7
Notations	$\Sigma_{c1}^{0\lambda'}$	$\Sigma_{c1}^{0\rho'}$	$\Sigma_{c1}^0$	$\Sigma_{c1}^{0\lambda'}$	$\Sigma_{c1}^{0\rho'}$	$\Sigma_{c0}^1$	$\Sigma_{c0}^{1\lambda'}$
Assignments	$\frac{1}{2}^+$ (2S)	$\frac{1}{2}^+$ (2S)	$\frac{3}{2}^+$ (1S)	$\frac{3}{2}^+$ (2S)	$\frac{3}{2}^+$ (2S)	$\frac{1}{2}^-$ (1P)	$\frac{1}{2}^-$ (2P)
Mass	2913	2913	2518	2967	2967	2823	3196
$\Lambda_c\pi^+$	71.70	$5.38\times 10^{-1}$	12.90	93.70	$1.75\times 10^{-4}$	282.70	6.96
$\Lambda_c\rho^+$	-	-	-	-	-	-	$1.26\times 10^{-9}$
$\Sigma_c^{++}\pi^0$	33.00	3.80	-	12.40	$8.26\times 10^{-1}$	$1.23\times 10^{-10}$	$8.93\times 10^{-10}$
$\Sigma_c^+\pi^+$	32.70	3.81	-	12.30	$8.33\times 10^{-1}$	$1.13\times 10^{-10}$	$3.03\times 10^{-9}$
$\Sigma_c^{*++}\pi^0$	9.28	1.73	-	38.00	4.78	$1.08\times 10^{-11}$	$3.55\times 10^{-9}$
$\Sigma_c^{*+}\pi^+$	9.28	1.73	-	38.00	4.78	$1.08\times 10^{-11}$	$3.55\times 10^{-9}$
$\Xi_c'^+K^+$	-	-	-	-	-	-	$1.50\times 10^{-10}$
$\Xi_c^+K^+$	-	-	-	$2.74\times 10^{-3}$	$1.35\times 10^{-3}$	-	2.31
$\Xi_c^{*+}K^+$	-	-	-	-	-	-	$1.41\times 10^{-10}$
$D^+p$	10.20	$3.50\times 10^{-1}$	-	18.80	1.26	100.30	8.09
$D^{*+}p$	-	-	-	1.77	$1.71\times 10^{-3}$	-	$1.38\times 10^{-8}$
$D^0\Delta^{++}$	-	-	-	-	-	-	$7.91\times 10^{-9}$
$D^+\Delta^+$	-	-	-	-	-	-	$2.36\times 10^{-9}$
$D_s\Sigma^+$	-	-	-	-	-	-	$1.51\times 10^{-11}$
$\Gamma_{total}$	166.16	11.96	12.90	214.97	12.48	383	17.36

TABLE IX: Two-body strong decays of  $\Sigma_c$  in MeV

N	1	2	3	4	5	6	7
Notations	$\Sigma_{c0}^{1\rho'}$	$\Sigma_{c1}^1$	$\Sigma_{c1}^{1\lambda'}$	$\Sigma_{c1}^{1\rho'}$	$\Sigma_{c1}^1$	$\Sigma_{c1}^{1\lambda'}$	$\Sigma_{c1}^{1\rho'}$
Assignments	$\frac{1}{2}^-$ (2P)	$\frac{1}{2}^-$ (1P)	$\frac{1}{2}^-$ (2P)	$\frac{1}{2}^-$ (2P)	$\frac{3}{2}^-$ (1P)	$\frac{3}{2}^-$ (2P)	$\frac{3}{2}^-$ (2P)
Mass	3196	2809	3185	3185	2829	3202	3202
$\Lambda_c \pi^+$	16.30	$5.85 \times 10^{-11}$	$4.53 \times 10^{-9}$	$7.91 \times 10^{-10}$	$2.22 \times 10^{-10}$	$4.45 \times 10^{-9}$	$4.27 \times 10^{-10}$
$\Lambda_c \rho^+$	$3.15 \times 10^{-9}$	-	3.42	57.8	-	3.69	52.80
$\Sigma_c^{++} \pi^0$	$1.25 \times 10^{-10}$	157	5.85	$2.90 \times 10^{-2}$	$9.92 \times 10^{-1}$	$2.97 \times 10^{-1}$	9.50
$\Sigma_c^+ \pi^+$	$2.36 \times 10^{-10}$	157	5.85	$3.20 \times 10^{-2}$	$9.71 \times 10^{-1}$	$2.95 \times 10^{-1}$	9.48
$\Sigma_c^{*++} \pi^0$	$8.65 \times 10^{-10}$	$3.90 \times 10^{-1}$	$2.84 \times 10^{-1}$	13.20	134	5.99	8.42
$\Sigma_c^{*+} \pi^+$	$8.65 \times 10^{-10}$	$3.90 \times 10^{-1}$	$2.84 \times 10^{-1}$	13.20	134	5.99	8.42
$\Xi_c'^+ K^+$	$1.40 \times 10^{-11}$	-	1.02	9.56	-	$1.36 \times 10^{-3}$	$2.07 \times 10^{-1}$
$\Xi_c^+ K^+$	6.68	-	$3.82 \times 10^{-10}$	$7.40 \times 10^{-11}$	-	$1.54 \times 10^{-10}$	$1.25 \times 10^{-10}$
$\Xi_c^{*+} K^+$	$3.04 \times 10^{-11}$	-	$1.07 \times 10^{-4}$	$2.60 \times 10^{-2}$	-	$7.15 \times 10^{-1}$	9.69
$D^+ p$	8.23	$1.26 \times 10^{-12}$	$8.45 \times 10^{-11}$	$4.65 \times 10^{-11}$	$7.76 \times 10^{-12}$	$6.24 \times 10^{-9}$	$1.80 \times 10^{-10}$
$D^{*+} p$	$7.51 \times 10^{-13}$	-	6.33	1.68	-	6.34	2.08
$D^0 \Delta^{++}$	$1.88 \times 10^{-11}$	-	$6.30 \times 10^{-2}$	$5.38 \times 10^{-1}$	-	10.4	$6.60 \times 10^{-1}$
$D^+ \Delta^+$	$2.52 \times 10^{-11}$	-	$1.90 \times 10^{-2}$	$1.63 \times 10^{-1}$	-	3.42	$2.50 \times 10^{-1}$
$D_s \Sigma^+$	$1.40 \times 10^{-11}$	-	2.95	1.68	-	$1.58 \times 10^{-3}$	$1.90 \times 10^{-2}$
$\Gamma_{total}$	31.21	314.78	26.07	97.91	269.96	37.14	101.53

TABLE X: Two-body strong decays of  $\Sigma_c$  in MeV

N	1	2	3	4	5	6
Notations	$\Sigma_{c2}^1$	$\Sigma_{c2}^{1\lambda'}$	$\Sigma_{c2}^{1\rho'}$	$\Sigma_{c2}^1$	$\Sigma_{c2}^{1\lambda'}$	$\Sigma_{c2}^{1\rho'}$
Assignments	$\frac{3}{2}^-$ (1P)	$\frac{3}{2}^-$ (2P)	$\frac{3}{2}^-$ (2P)	$\frac{5}{2}^-$ (1P)	$\frac{5}{2}^-$ (2P)	$\frac{5}{2}^-$ (2P)
Mass	2806	3179	3179	2835	3207	3207
$\Lambda_c \pi^+$	13.60	2.06	33.40	18.70	2.49	35.0
$\Lambda_c \rho^+$	-	$1.70 \times 10^{-2}$	8.99	-	$3.70 \times 10^{-2}$	14.5
$\Sigma_c^{++} \pi^0$	1.13	$4.36 \times 10^{-1}$	15.57	$8.70 \times 10^{-1}$	$2.46 \times 10^{-1}$	7.75
$\Sigma_c^+ \pi^+$	1.11	$4.33 \times 10^{-1}$	5.53	$8.50 \times 10^{-1}$	$2.46 \times 10^{-1}$	7.74
$\Sigma_c^{*++} \pi^0$	$2.95 \times 10^{-1}$	$2.41 \times 10^{-1}$	11.51	$9.70 \times 10^{-1}$	$4.93 \times 10^{-1}$	20.70
$\Sigma_c^{*+} \pi^+$	$2.95 \times 10^{-1}$	$2.41 \times 10^{-1}$	11.51	$9.70 \times 10^{-1}$	$4.93 \times 10^{-1}$	20.70
$\Xi_c'^+ K^+$	-	$1.29 \times 10^{-3}$	$2.30 \times 10^{-1}$	-	$1.24 \times 10^{-3}$	$1.83 \times 10^{-1}$
$\Xi_c^+ K^+$	-	$1.90 \times 10^{-2}$	1.75	-	$3.00 \times 10^{-2}$	2.33
$\Xi_c^{*+} K^+$	-	$6.28 \times 10^{-5}$	$1.6 \times 10^{-2}$	-	$4.96 \times 10^{-4}$	$1.07 \times 10^{-1}$
$D^+ p$	-	0.854	1.95	$5.70 \times 10^{-2}$	1.05	1.99
$D^{*+} p$	-	$3.60 \times 10^{-1}$	2.66	-	$4.98 \times 10^{-1}$	3.16
$D^0 \Delta^{++}$	-	$4.80 \times 10^{-2}$	$4.30 \times 10^{-1}$	-	$1.43 \times 10^{-1}$	1.08
$D^+ \Delta^+$	-	$1.40 \times 10^{-2}$	$1.30 \times 10^{-1}$	-	$4.30 \times 10^{-2}$	$3.40 \times 10^{-1}$
$D_s \Sigma^+$	-	$4.55 \times 10^{-4}$	$6.25 \times 10^{-3}$	-	$1.67 \times 10^{-3}$	$2.00 \times 10^{-2}$
$\Gamma_{total}$	19.13	4.72	93.68	22.42	5.77	115.60

TABLE XI: Two-body strong decays of  $\Sigma_b$  in MeV

N	1	2	3	4	5	6	7
Notations	$\Sigma_{b1}^{0\lambda'}$	$\Sigma_{b1}^{0\rho'}$	$\Sigma_{b1}^0$	$\Sigma_{b1}^{0\lambda'}$	$\Sigma_{b1}^{0\rho'}$	$\Sigma_{b0}^1$	$\Sigma_{b0}^{1\lambda'}$
Assignments	$\frac{1}{2}^+$ (2S)	$\frac{1}{2}^+$ (2S)	$\frac{3}{2}^+$ (1S)	$\frac{3}{2}^+$ (2S)	$\frac{3}{2}^+$ (2S)	$\frac{1}{2}^-$ (1P)	$\frac{1}{2}^-$ (2P)
Mass	6225	6225	5835	6246	6246	6113	6447
$\Lambda_b\pi^+$	88.80	$3.05\times 10^{-1}$	14.0	100	$4.50\times 10^{-2}$	316	8.23
$\Lambda_b\rho^+$	-	-	-	-	-	-	$3.42\times 10^{-9}$
$\Sigma_b^+\pi^0$	28.40	4.09	-	8.67	1.04	$3.64\times 10^{-12}$	$2.60\times 10^{-9}$
$\Sigma_b^0\pi^+$	28.20	4.09	-	8.59	1.04	$6.54\times 10^{-12}$	$2.56\times 10^{-9}$
$\Sigma_b^{*+}\pi^0$	11.80	1.96	-	36.3	5.13	$6.60\times 10^{-13}$	$1.62\times 10^{-9}$
$\Sigma_b^{*0}\pi^+$	11.80	1.96	-	36.3	5.13	$6.60\times 10^{-13}$	$1.62\times 10^{-9}$
$\Xi_b'^+K^+$	-	-	-	-	-	-	-
$\Xi_b^+K^+$	-	-	-	-	-	-	2.31
$\overline{B}^0p$	$3.06\times 10^{-1}$	$3.19\times 10^{-3}$	-	2.46	$4.70\times 10^{-2}$	-	12.4
$\overline{B}^{*0}p$	-	-	-	-	-	-	$7.11\times 10^{-11}$
$\Gamma_{total}$	169.31	12.41	14.00	189.91	12.43	316.00	22.94

TABLE XII: Two-body strong decays of  $\Sigma_b$  in MeV

N	1	2	3	4	5	6	7
Notations	$\Sigma_{b0}^{1\rho'}$	$\Sigma_{b1}^1$	$\Sigma_{b1}^{1\lambda'}$	$\Sigma_{b1}^{1\rho'}$	$\Sigma_{b1}^1$	$\Sigma_{b1}^{1\lambda'}$	$\Sigma_{b1}^{1\rho'}$
Assignments	$\frac{1}{2}^-$ (2P)	$\frac{1}{2}^-$ (1P)	$\frac{1}{2}^-$ (2P)	$\frac{1}{2}^-$ (2P)	$\frac{3}{2}^-$ (1P)	$\frac{3}{2}^-$ (2P)	$\frac{3}{2}^-$ (2P)
Mass	6447	6107	6442	6442	6116	6450	6450
$\Lambda_b\pi^+$	16.70	$9.39\times 10^{-11}$	$5.50\times 10^{-9}$	$1.06\times 10^{-9}$	-	$6.05\times 10^{-9}$	$1.37\times 10^{-9}$
$\Lambda_b\rho^+$	$1.87\times 10^{-10}$	-	2.47	83.4	-	2.71	83.3
$\Sigma_b^+\pi^0$	$4.47\times 10^{-10}$	139	6.45	2.08	$3.52\times 10^{-1}$	$1.80\times 10^{-1}$	7.89
$\Sigma_b^0\pi^+$	$4.82\times 10^{-10}$	138	6.45	2.14	$3.40\times 10^{-1}$	$1.79\times 10^{-1}$	7.86
$\Sigma_b^{*+}\pi^0$	$6.71\times 10^{-10}$	$3.59\times 10^{-1}$	$2.66\times 10^{-1}$	13.4	132	6.53	9.90
$\Sigma_b^{*0}\pi^+$	$6.71\times 10^{-10}$	$3.59\times 10^{-1}$	$2.66\times 10^{-1}$	13.4	132	6.53	9.90
$\Xi_b'^+K^+$	$1.40\times 10^{-12}$	-	$9.70\times 10^{-2}$	1.92	-	$1.43\times 10^{-6}$	$3.77\times 10^{-4}$
$\Xi_b^+K^+$	12.40	-	$1.54\times 10^{-10}$	$1.84\times 10^{-11}$	-	$1.87\times 10^{-7}$	$2.56\times 10^{-11}$
$\overline{B}^0p$	4.60	-	$2.62\times 10^{-10}$	$1.51\times 10^{-10}$	-	$4.69\times 10^{-10}$	$5.82\times 10^{-11}$
$\overline{B}^{*0}p$	$7.65\times 10^{-11}$	-	8.39	1.67	-	8.41	1.96
$\Gamma_{total}$	33.70	277.72	24.39	118.01	264.69	24.54	120.81

TABLE XIII: Two-body strong decays of  $\Sigma_b$  in MeV

N	1	2	3	4	5	6
Notations	$\Sigma_{b2}^1$	$\Sigma_{b2}^{1\lambda'}$	$\Sigma_{b2}^{1\rho'}$	$\Sigma_{b2}^1$	$\Sigma_{b2}^{1\lambda'}$	$\Sigma_{b2}^{1\rho'}$
Assignments	$\frac{3}{2}^-$ (1P)	$\frac{3}{2}^-$ (2P)	$\frac{3}{2}^-$ (2P)	$\frac{5}{2}^-$ (1P)	$\frac{5}{2}^-$ (2P)	$\frac{5}{2}^-$ (2P)
Mass	6098	6439	6439	6119	6452	6452
$\Lambda_b \pi^+$	14.10	2.34	38.6	16.7	2.60	39.7
$\Lambda_b \rho^+$	-	$1.15 \times 10^{-3}$	1.53	-	$2.62 \times 10^{-3}$	2.86
$\Sigma_b^+ \pi^0$	$4.81 \times 10^{-1}$	$2.87 \times 10^{-1}$	13.30	$3.00 \times 10^{-1}$	$1.47 \times 10^{-1}$	6.39
$\Sigma_b^0 \pi^+$	$4.62 \times 10^{-1}$	$2.84 \times 10^{-1}$	13.20	$2.91 \times 10^{-1}$	$1.46 \times 10^{-1}$	6.36
$\Sigma_b^{*+} \pi^0$	$2.99 \times 10^{-1}$	$2.31 \times 10^{-1}$	11.8	$6.80 \times 10^{-1}$	$4.19 \times 10^{-1}$	20.00
$\Sigma_b^{*0} \pi^+$	$2.99 \times 10^{-1}$	$2.31 \times 10^{-1}$	11.8	$6.80 \times 10^{-1}$	$4.19 \times 10^{-1}$	20.00
$\Xi_b'^+ K^+$	-	-	-	-	$8.88 \times 10^{-7}$	$5.02 \times 10^{-4}$
$\Xi_b^+ K^+$	-	$8.11 \times 10^{-3}$	1.00	-	$1.10 \times 10^{-2}$	1.24
$\overline{B}^0 p$	-	$5.13 \times 10^{-1}$	1.51	-	$6.03 \times 10^{-1}$	1.61
$\overline{B}^{*0} p$	-	$4.09 \times 10^{-1}$	2.42	-	$5.00 \times 10^{-1}$	2.71
$\Gamma_{total}$	15.64	4.30	95.16	18.65	4.85	100.87

TABLE XIV: Two-body strong decays of  $\Omega_c$  in MeV

N	1	2	3	4	5	6
Notations	$\Omega_{c1}^{0\lambda'}$	$\Omega_{c1}^{0\rho'}$	$\Omega_{c1}^{0\lambda'}$	$\Omega_{c1}^{0\rho'}$	$\Omega_{c0}^1$	$\Omega_{c0}^{1\lambda'}$
Assignments	$\frac{1}{2}^+$ (2S)	$\frac{1}{2}^+$ (2S)	$\frac{3}{2}^+$ (2S)	$\frac{3}{2}^+$ (2S)	$\frac{1}{2}^-$ (1P)	$\frac{1}{2}^-$ (2P)
Mass	3120	3120	3197	3197	3057	3426
$\Xi_c^+ K^-$	14.40	2.03	28.9	1.38	183	4.79
$\Xi_c^+ K^{*-}$	-	-	-	-	-	$1.11 \times 10^{-8}$
$\Xi_c^0 \overline{K}^0$	13.50	2.04	27.81	1.47	181	4.83
$\Xi_c^0 \overline{K}^{*0}$	-	-	-	-	-	$3.54 \times 10^{-9}$
$\Xi_c'^+ K^-$	2.77	1.01	3.28	$6.40 \times 10^{-1}$	-	$7.45 \times 10^{-10}$
$\Xi_c^{*+} K^-$	-	-	3.17	1.18	-	$1.15 \times 10^{-10}$
$\Xi_c'^0 \overline{K}^0$	2.29	$8.70 \times 10^{-1}$	3.07	$6.30 \times 10^{-1}$	-	$1.51 \times 10^{-9}$
$\Xi_c^{*0} \overline{K}^0$	-	-	2.69	1.03	-	$5.34 \times 10^{-10}$
$\Xi^0 D^0$	-	-	$5.60 \times 10^{-1}$	$2.31 \times 10^{-3}$	-	$9.90 \times 10^{-10}$
$\Xi^- D^+$	-	-	$9.00 \times 10^{-2}$	$1.67 \times 10^{-4}$	-	$3.80 \times 10^{-10}$
$\Xi^0 D^{*0}$	-	-	-	-	-	1.85
$\Xi^- D^{*+}$	-	-	-	-	-	1.77
$\Gamma_{total}$	32.96	5.95	78.16	6.33	364.00	13.24

TABLE XV: Two-body strong decays of  $\Omega_c$  in MeV

N	1	2	3	4	5	6	7
Notations	$\Omega_{c0}^{1\rho'}$	$\Omega_{c1}^1$	$\Omega_{c1}^{1\lambda'}$	$\Omega_{c1}^{1\rho'}$	$\Omega_{c1}^1$	$\Omega_{c1}^{1\lambda'}$	$\Omega_{c1}^{1\rho'}$
Assignments	$\frac{1}{2}^-$ (2P)	$\frac{1}{2}^-$ (1P)	$\frac{1}{2}^-$ (2P)	$\frac{1}{2}^-$ (2P)	$\frac{3}{2}^-$ (1P)	$\frac{3}{2}^-$ (2P)	$\frac{3}{2}^-$ (2P)
Mass	3426	3000	3416	3416	3050	3431	3431
$\Xi_c^+ K^-$	2.25	$1.30 \times 10^{-11}$	$1.38 \times 10^{-9}$	$2.89 \times 10^{-9}$	$2.06 \times 10^{-10}$	$7.89 \times 10^{-10}$	$2.27 \times 10^{-9}$
$\Xi_c^+ K^{*-}$	$7.90 \times 10^{-10}$	-	1.21	39.60	-	1.41	38.9
$\Xi_c^0 \bar{K}^0$	1.95	$8.76 \times 10^{-12}$	$1.25 \times 10^{-9}$	$9.24 \times 10^{-11}$	$7.88 \times 10^{-11}$	$4.80 \times 10^{-10}$	$2.49 \times 10^{-9}$
$\Xi_c^0 \bar{K}^{*0}$	$1.60 \times 10^{-9}$	-	1.18	39.6	-	1.38	39.10
$\Xi_c'^+ K^-$	$9.67 \times 10^{-11}$	-	3.52	$8.94 \times 10^{-1}$	-	$1.14 \times 10^{-1}$	4.61
$\Xi_c^{*'+} K^-$	$5.67 \times 10^{-10}$	-	$7.25 \times 10^{-2}$	4.95	-	3.44	7.30
$\Xi_c'^0 \bar{K}^0$	$3.15 \times 10^{-10}$	-	3.53	1.05	-	$1.09 \times 10^{-1}$	4.53
$\Xi_c^{*'0} \bar{K}^0$	$4.88 \times 10^{-10}$	-	$6.94 \times 10^{-2}$	4.83	-	3.43	7.51
$\Xi^0 D^0$	$9.84 \times 10^{-12}$	-	11.0	2.602	-	$3.40 \times 10^{-1}$	1.19
$\Xi^- D^+$	$5.07 \times 10^{-11}$	-	11.1	2.012	-	$3.02 \times 10^{-1}$	1.14
$\Xi^0 D^{*0}$	2.69	-	$1.56 \times 10^{-1}$	2.097	-	$1.16 \times 10^{-1}$	1.42
$\Xi^- D^{*+}$	2.38	-	$1.18 \times 10^{-1}$	1.67	-	$9.10 \times 10^{-2}$	1.18
$\Gamma_{total}$	9.27	$2.18 \times 10^{-11}$	31.96	99.31	$2.85 \times 10^{-10}$	10.73	106.88

TABLE XVI: Two-body strong decays of  $\Omega_c$  in MeV

N	1	2	3	4	5	6
Notations	$\Omega_{c2}^1$	$\Omega_{c2}^{1\lambda'}$	$\Omega_{c2}^{1\rho'}$	$\Omega_{c2}^1$	$\Omega_{c2}^{1\lambda'}$	$\Omega_{c2}^{1\rho'}$
Assignments	$\frac{3}{2}^-$ (1P)	$\frac{3}{2}^-$ (2P)	$\frac{3}{2}^-$ (2P)	$\frac{5}{2}^-$ (1P)	$\frac{5}{2}^-$ (2P)	$\frac{5}{2}^-$ (2P)
Mass	3066	3411	3411	3090	3435	3435
$\Xi_c^+ K^-$	$5.99 \times 10^{-1}$	0.634	15.80	1.35	$7.80 \times 10^{-1}$	17.0
$\Xi_c^+ K^{*-}$	-	$5.81 \times 10^{-4}$	$7.68 \times 10^{-1}$	-	$2.29 \times 10^{-3}$	2.04
$\Xi_c^0 \bar{K}^0$	$4.80 \times 10^{-1}$	$6.10 \times 10^{-1}$	15.6	1.15	$7.51 \times 10^{-1}$	16.8
$\Xi_c^0 \bar{K}^{*0}$	-	$5.07 \times 10^{-4}$	$6.92 \times 10^{-1}$	-	$2.15 \times 10^{-3}$	1.91
$\Xi_c'^+ K^-$	-	$1.64 \times 10^{-1}$	7.43	-	$9.50 \times 10^{-2}$	3.77
$\Xi_c^{*+} K^-$	-	$6.10 \times 10^{-2}$	4.27	-	$1.32 \times 10^{-1}$	8.08
$\Xi_c^{\prime 0} \bar{K}^0$	-	$1.57 \times 10^{-1}$	7.27	-	$9.10 \times 10^{-2}$	3.70
$\Xi_c^{*0} \bar{K}^0$	-	$5.80 \times 10^{-2}$	4.16	-	$1.26 \times 10^{-1}$	7.90
$\Xi^0 D^0$	-	$4.88 \times 10^{-1}$	1.95	-	$2.84 \times 10^{-1}$	$9.67 \times 10^{-1}$
$\Xi^- D^+$	-	$4.28 \times 10^{-1}$	1.84	-	$2.52 \times 10^{-1}$	$9.26 \times 10^{-1}$
$\Xi^0 D^{*0}$	-	16.0	6.67	-	$5.10 \times 10^{-2}$	$6.12 \times 10^{-1}$
$\Xi^- D^{*+}$	-	15.4	7.62	-	$4.00 \times 10^{-2}$	$5.12 \times 10^{-1}$
$\Gamma_{total}$	1.08	34.00	74.07	2.50	2.61	64.22

TABLE XVII: Two-body strong decays of  $\Omega_c$  in MeV

N	1	2	3	4	5	6
Notations	$\Omega_{c1}^2$	$\Omega_{c1}^2$	$\Omega_{c2}^2$	$\Omega_{c2}^2$	$\Omega_{c3}^2$	$\Omega_{c3}^2$
Assignments	$\frac{1}{2}^+$ (1D)	$\frac{3}{2}^+$ (1D)	$\frac{3}{2}^+$ (1D)	$\frac{5}{2}^+$ (1D)	$\frac{5}{2}^+$ (1D)	$\frac{7}{2}^+$ (1D)
Mass	3304	3313	3304	3314	3304	3315
$\Xi_c^+ K^-$	10.01	10.12	-	-	1.04	1.17
$\Xi_c^0 \bar{K}^0$	9.98	10.97	-	-	$9.82 \times 10^{-1}$	1.11
$\Xi_c'^+ K^-$	2.55	$6.61 \times 10^{-1}$	5.74	$1.54 \times 10^{-1}$	$1.51 \times 10^{-1}$	$1.11 \times 10^{-1}$
$\Xi_c^{*+} K^-$	$8.00 \times 10^{-1}$	2.15	$7.69 \times 10^{-1}$	4.70	$4.00 \times 10^{-2}$	$7.01 \times 10^{-2}$
$\Xi_c^{\prime 0} \bar{K}^0$	2.51	$6.52 \times 10^{-1}$	5.65	$1.44 \times 10^{-1}$	$1.41 \times 10^{-1}$	$9.43 \times 10^{-2}$
$\Xi_c^{*0} \bar{K}^0$	$7.77 \times 10^{-1}$	2.09	$7.45 \times 10^{-1}$	4.58	$3.64 \times 10^{-2}$	$6.42 \times 10^{-2}$
$\Xi^0 D^0$	2.23	$5.97 \times 10^{-1}$	5.02	$5.53 \times 10^{-2}$	$4.90 \times 10^{-2}$	-
$\Xi^- D^+$	2.02	$5.48 \times 10^{-1}$	4.56	$4.12 \times 10^{-2}$	$3.54 \times 10^{-2}$	-
$\Gamma_{total}$	30.87	27.73	22.48	9.64	2.48	2.62



TABLE XVIII: Two-body strong decays of  $\Omega_b$  in MeV

N	1	2	3	4	5	6
Notations	$\Omega_{b1}^{0\lambda'}$	$\Omega_{b1}^{0\rho'}$	$\Omega_{b1}^{0\lambda'}$	$\Omega_{b1}^{0\rho'}$	$\Omega_{b0}^1$	$\Omega_{b0}^{1\lambda'}$
Assignments	$\frac{1}{2}^+$ (2S)	$\frac{1}{2}^+$ (2S)	$\frac{3}{2}^+$ (2S)	$\frac{3}{2}^+$ (2S)	$\frac{1}{2}^-$ (1P)	$\frac{1}{2}^-$ (2P)
Mass	6446	6446	6466	6466	6334	6662
$\Xi_b^0 K^-$	258	2.23	25.30	2.03	169	5.83
$\Xi_b^- \bar{K}^0$	235	2.29	23.00	2.16	155	5.91
$\Xi_b^{\prime 0} K^-$	11.30	$3.30 \times 10^{-1}$	$6.00 \times 10^{-1}$	$2.30 \times 10^{-1}$	-	$2.21 \times 10^{-10}$
$\Xi_b^{*\prime 0} K^-$	-	-	$3.30 \times 10^{-2}$	$1.60 \times 10^{-2}$	-	$8.14 \times 10^{-10}$
$\Xi_b^{\prime -} \bar{K}^0$	7.03	$2.10 \times 10^{-1}$	$4.87 \times 10^{-1}$	$1.90 \times 10^{-1}$	-	$9.17 \times 10^{-11}$
$\Xi_b^{*\prime -} \bar{K}^0$	-	-	-	-	-	$1.19 \times 10^{-9}$
$\Xi^0 B^-$	-	-	-	0	-	$9.04 \times 10^{-11}$
$\Xi^- \bar{B}^0$	-	-	-	0	-	$4.98 \times 10^{-9}$
$\Xi^0 B^{*-}$	-	-	-	-	-	1.45
$\Xi^- \bar{B}^{*0}$	-	-	-	-	-	1.22
$\Gamma_{total}$	511.30	5.06	49.42	4.63	324	14.41

TABLE XIX: Two-body strong decays of  $\Omega_b$  in MeV

N	1	2	3	4	5	6	7
Notations	$\Omega_{b0}^{1\rho'}$	$\Omega_{b1}^1$	$\Omega_{b1}^{1\lambda'}$	$\Omega_{b1}^{1\rho'}$	$\Omega_{b1}^1$	$\Omega_{b1}^{1\lambda'}$	$\Omega_{b1}^{1\rho'}$
Assignments	$\frac{1}{2}^-$ (2P)	$\frac{1}{2}^-$ (1P)	$\frac{1}{2}^-$ (2P)	$\frac{1}{2}^-$ (2P)	$\frac{3}{2}^-$ (1P)	$\frac{3}{2}^-$ (2P)	$\frac{3}{2}^-$ (2P)
Mass	6662	6316	6658	6658	6330	6664	6664
$\Xi_b^0 K^-$	$5.60 \times 10^{-1}$	$2.76 \times 10^{-11}$	$6.27 \times 10^{-8}$	$8.94 \times 10^{-11}$	$6.08 \times 10^{-12}$	$1.43 \times 10^{-9}$	$1.27 \times 10^{-10}$
$\Xi_b^- \bar{K}^0$	$2.50 \times 10^{-1}$	$1.13 \times 10^{-11}$	$1.55 \times 10^{-8}$	$1.78 \times 10^{-10}$	$2.35 \times 10^{-11}$	$2.83 \times 10^{-9}$	$1.69 \times 10^{-10}$
$\Xi_b^{\prime 0} K^-$	$1.68 \times 10^{-10}$	-	3.69	7.33	-	$3.90 \times 10^{-2}$	2.73
$\Xi_b^{*\prime 0} K^-$	$1.56 \times 10^{-10}$	-	$3.80 \times 10^{-2}$	3.44	-	3.47	12.70
$\Xi_b^{\prime -} \bar{K}^0$	$2.04 \times 10^{-10}$	-	3.68	7.76	-	$3.70 \times 10^{-2}$	2.65
$\Xi_b^{*\prime -} \bar{K}^0$	$2.25 \times 10^{-10}$	-	$3.60 \times 10^{-2}$	3.30	-	3.46	13.10
$\Xi^0 B^-$	$1.18 \times 10^{-11}$	-	13.90	$7.70 \times 10^{-1}$	-	$3.50 \times 10^{-2}$	$2.50 \times 10^{-1}$
$\Xi^- \bar{B}^0$	$3.01 \times 10^{-12}$	-	13.30	1.16	-	$2.60 \times 10^{-2}$	$1.90 \times 10^{-1}$
$\Xi^0 B^{*-}$	1.11	-	$6.25 \times 10^{-3}$	$9.50 \times 10^{-2}$	-	$6.51 \times 10^{-3}$	$9.50 \times 10^{-2}$
$\Xi^- \bar{B}^{*0}$	1.01	-	$1.82 \times 10^{-3}$	$2.90 \times 10^{-2}$	-	$2.75 \times 10^{-3}$	$4.80 \times 10^{-2}$
$\Gamma_{total}$	2.93	$3.89 \times 10^{-11}$	34.65	23.88	$2.96 \times 10^{-11}$	7.08	31.76

TABLE XX: Two-body strong decays of  $\Omega_b$  in MeV

N	1	2	3	4	5	6
Notations	$\Omega_{b2}^1$	$\Omega_{b2}^{1\lambda'}$	$\Omega_{b2}^{1\rho'}$	$\Omega_{b2}^1$	$\Omega_{b2}^{1\lambda'}$	$\Omega_{b2}^{1\rho'}$
Assignments	$\frac{3}{2}^-$ (1P)	$\frac{3}{2}^-$ (2P)	$\frac{3}{2}^-$ (2P)	$\frac{5}{2}^-$ (1P)	$\frac{5}{2}^-$ (2P)	$\frac{5}{2}^-$ (2P)
Mass	6340	6655	6655	6350	6666	6666
$\Xi_b^0 K^-$	$1.70 \times 10^{-1}$	$5.60 \times 10^{-1}$	16.50	$3.50 \times 10^{-1}$	$6.30 \times 10^{-1}$	17.30
$\Xi_b^- \bar{K}^0$	$8.10 \times 10^{-2}$	$5.10 \times 10^{-1}$	15.90	$2.00 \times 10^{-1}$	$5.70 \times 10^{-1}$	16.70
$\Xi_b^{\prime 0} K^-$	-	$6.10 \times 10^{-2}$	4.49	-	$3.30 \times 10^{-2}$	2.23
$\Xi_b^{*\prime 0} K^-$	-	$3.20 \times 10^{-2}$	2.98	-	$6.20 \times 10^{-2}$	5.31
$\Xi_b^{\prime -} \bar{K}^0$	-	$5.80 \times 10^{-2}$	4.35	-	$3.10 \times 10^{-2}$	2.16
$\Xi_b^{*\prime -} \bar{K}^0$	-	$3.00 \times 10^{-2}$	2.86	-	$5.80 \times 10^{-2}$	5.11
$\Xi_b^0 B^-$	-	$4.40 \times 10^{-2}$	$3.30 \times 10^{-1}$	-	$3.00 \times 10^{-2}$	$2.10 \times 10^{-1}$
$\Xi_b^- \bar{B}^0$	-	$3.10 \times 10^{-2}$	$2.0 \times 10^{-1}$	-	$2.30 \times 10^{-2}$	$1.70 \times 10^{-1}$
$\Xi_b^0 B^{*-}$	-	12.10	9.58	-	$3.19 \times 10^{-3}$	$4.60 \times 10^{-2}$
$\Xi_b^- \bar{B}^{*0}$	-	9.00	8.23	-	$1.46 \times 10^{-3}$	$2.20 \times 10^{-2}$
$\Gamma_{total}$	$2.50 \times 10^{-1}$	22.43	65.47	$5.50 \times 10^{-1}$	1.44	49.26

TABLE XXI: Two-body strong decays of  $\Omega_b$  in MeV

N	1	2	3	4	5	6
Notations	$\Omega_{b1}^2$	$\Omega_{b1}^2$	$\Omega_{b2}^2$	$\Omega_{b2}^2$	$\Omega_{b3}^2$	$\Omega_{b3}^2$
Assignments	$\frac{1}{2}^+$ (1D)	$\frac{3}{2}^+$ (1D)	$\frac{3}{2}^+$ (1D)	$\frac{5}{2}^+$ (1D)	$\frac{5}{2}^+$ (1D)	$\frac{7}{2}^+$ (1D)
Mass	6556	6561	6556	6561	6556	6562
$\Xi_b^0 K^-$	10.82	10.95	-	-	$7.83 \times 10^{-1}$	$8.51 \times 10^{-1}$
$\Xi_b^- \bar{K}^0$	10.95	10.74	-	-	$6.88 \times 10^{-1}$	$7.51 \times 10^{-1}$
$\Xi_b^{\prime 0} K^-$	1.61	$4.23 \times 10^{-1}$	3.62	$2.68 \times 10^{-2}$	$2.65 \times 10^{-2}$	$1.77 \times 10^{-2}$
$\Xi_b^{*\prime 0} K^-$	$5.12 \times 10^{-1}$	1.38	$4.73 \times 10^{-1}$	2.99	-	$1.64 \times 10^{-2}$
$\Xi_b^{\prime -} \bar{K}^0$	1.55	$4.08 \times 10^{-1}$	3.49	$2.40 \times 10^{-2}$	$2.36 \times 10^{-2}$	$1.58 \times 10^{-2}$
$\Xi_b^{*\prime -} \bar{K}^0$	$4.82 \times 10^{-1}$	1.30	$4.44 \times 10^{-1}$	2.82	-	$1.40 \times 10^{-2}$
$\Gamma_{total}$	25.57	25.20	8.03	5.86	1.53	1.67